

## Mapping interactions between geology, subsurface resource exploitation and urban development in transforming cities using InSAR Persistent Scatterers: Two decades of change in Florence, Italy

Fabio Pratesi <sup>a, b,\*</sup>, Deodato Tapete <sup>c</sup>, Chiara Del Ventisette <sup>a</sup>, Sandro Moretti <sup>a</sup>

<sup>a</sup> University of Florence, Earth Sciences Department, Via La Pira, 4, 50121, Firenze, Italy

<sup>b</sup> University of Florence, Department of Civil and Environmental Engineering, Via di S. Marta, 3, 50139, Firenze, Italy

<sup>c</sup> British Geological Survey, Natural Environment Research Council, Nicker Hill, Keyworth, NG12 5GG, United Kingdom

### ARTICLE INFO

#### Article history:

Received 18 October 2015

Received in revised form

4 September 2016

Accepted 13 September 2016

Available online 20 October 2016

#### Keywords:

Urban dynamics

Urban growth

Structural stability

Urban geohazards

Space-borne InSAR

Florence

### ABSTRACT

Urban expansion and city transformation are increasing reality across the world. Now more than ever it is essential to understand and map at the appropriate scale the processes happening along the verticality and horizontality of cities, to gather robust evidence underpinning strategies for sustainable management of the built environment. This paper explores how established techniques of Persistent Scatterer Interferometry (PSI) can be shaped into a novel dedicated procedure to detect vertical and horizontal urban dynamics including: use and re-use of urban space (new building construction, intentional demolition, renovation projects); exploitation of groundwater resources (induced land subsidence); interactions between new foundations, superficial deposits and bedrock geology (settlement of recent buildings); ground and slope instability affecting settled buildings; susceptibility of heritage assets to structural damages; baseline characterisation prior to planned major infrastructure construction (tunnelling and transportation networks). Florence, central Italy, is used as a demonstration site. This city includes UNESCO World Heritage List historic centre, 20<sup>th</sup>-century residential, industrial and peri-urban quarters, and is currently in transition to metropolitan area of over 1 million of inhabitants. Velocity decomposition maps were generated based on millimetre-precise estimates of surface displacements retrieved from PSI processing of the full archives of satellite C-band radar images, including 79 ERS-1/2 descending (1992–2000), 70 ENVISAT ASAR ascending and descending (2003–2010) and 101 RADARSAT-1 ascending and descending (2003–2007). 12 macropatterns and 84 micropatterns in the final map of alert areas highlight a dualism which reflects the physical and urban geography of Florence. North-western and south-western quarters show hot spots of new building construction and regeneration projects for residential, business and tertiary service purposes, alongside issues due to groundwater exploitation and induced land subsidence up to 30–40 mm/yr. Local interactions with underlying geology and natural slope instability processes predominate in the southern and north-eastern sectors. At local scale, stable condition was found for the heritage assets and buildings located along the tracks of the planned subway railway and tramway, with motion rates averagely within ±1.5 mm/yr and localised deformation only up to –3.5 mm/yr. Structural assessment based on future PSI monitoring campaign will benefit of this baseline characterisation.

© 2016 The Authors. Published by Elsevier Ltd. This is an open access article under the CC BY-NC-ND license (<http://creativecommons.org/licenses/by-nc-nd/4.0/>).

## 1. Introduction

Cities are vital anthropogenic settings changing in time in

response to the needs of the living communities, and their use of the local natural environment and resources. Processes involved include: the interaction with the bedrock geology and superficial deposits to place the foundations of buildings; the use or even reshaping of the geomorphologic and topographic setting to create space for new constructions, infrastructure and tunnelling; and the exploitation of the subsurface and groundwater to supply building materials and water.

\* Corresponding author. University of Florence, Earth Sciences Department, Via La Pira, 4, 50121, Firenze, Italy.

E-mail address: [ing.pratesi@gmail.com](mailto:ing.pratesi@gmail.com) (F. Pratesi).

## Key terms and acronyms

Alert area	Classified pattern of moving PS and mapped area of observed instability
$I_{CC,a}$	Index of conservation criticality expressing the (in) stability condition of the area surrounding a building
$I_{CC,o}$	Index of conservation criticality of a building
$I_{CI}$	Index of completeness of information expressing PS degree of coverage over a building
Localised deformation	Group of few to single moving PS that generally corresponds with localised damaged portions of a building
Macropattern	Homogeneous group of moving PS that cover a wide area, e.g. a sector of a city
Map of alert areas	Map of the urban dynamics individuated through the analysis of PS displacement maps
Map of urban evolution	Map of the expansion/transformation of urban areas as revealed by the comparison of multi-temporal PS displacement maps
Micropattern	Homogeneous group of moving PS that include single buildings or small groups of buildings
PS	Persistent Scatterer, radar target on the ground, the displacement of which is estimated
$PS_A$	PS displacement map based on radar acquisitions in the period A
$PS_B$	PS displacement map based on radar acquisitions in the period B
PSI	Persistent Scatterer Interferometry
Velocity decomposition map	Displacement map where PS are classified by velocity
$V_{lim}$	Velocity limit used to discriminate between moving and stable PS

using radar data for urban geographic applications (Stabel & Fischer, 2001; Zong-Guo & Henderson, 1997), this paper aims to propose a multi-scale and multi-temporal approach based on the use of Interferometric Synthetic Aperture Radar (InSAR), particularly Persistent Scatterer Interferometry (PSI), to detect and map the effects visible at the surface of both vertical and horizontal urban dynamics.

There is a plethora of published research showing how the displacement time series obtained from PSI can be used valuably as surface measurements to infer impact of geological and human-induced processes in wide urban areas (e.g. Chatterjee et al., 2006; Terranova, Ventura, & Vilardo, 2015) and historic cities (e.g. Cigna, Lasaponara, Masini, Milillo, & Tapete, 2014c, 2012; Stramondo et al., 2008). More recent contributions have explored how to exploit the wide availability of more than 20 years of satellite radar observations from past (e.g. ERS-1/2, ENVISAT ASAR and RADARSAT-1) and new missions (e.g. RADARSAT-2, COSMO-SkyMed) as legacy datasets and increasing catalogues, respectively, to monitor the evolution of metropolises and big cities (Cigna, Jordan, Bateson, McCormack, & Roberts, 2014b; Samsonov et al., 2014). But there has not been so far research dedicated on developing a workflow to: classify PSI estimates; generate a mapping product at city scale showing the spatial distribution of the patterns observed; use this map to investigate the geography of urban dynamics through time; and downscale at the level of individual buildings attributing the observed pattern to the causative factors.

It is this method and how to use it in a complex and transforming urban environment that form the focus of this paper. A catalogue of urban dynamics is discussed through the demonstration site of the Municipality of Florence. This is among the top-10 most populated cities in Italy and, at present, an example of coexistence of two urban souls: a historic city centre inscribed in the UNESCO World Heritage List, and an expanding metropolitan area to over 1 million of inhabitants. The complexity of the transition that Florence is currently experiencing is also due to the wide range of urban dynamics involved, the variety of building categories and heritage assets, and the spectrum of geohazards affecting the built environment. To capture these multiple processes in both spatial and temporal dimensions we used a range of PSI datasets providing a consistent coverage of the city dynamics from 1992 to 2010.

Although they mostly affect the vertical dimension of cities, these urban dynamics are also manifestations along the horizontality due to the processes of urban expansion, building construction and renovation, development of vacant and derelict land.

At present, several cities in both developed and developing countries experience these dynamics of transformation (e.g. Romero-Lankao & Dodman, 2011). In historic urban centres, this transition typically adds onto existing issues related to structural and/or geological instability, maintenance of the built heritage and management of infrastructures.

Mapping urban dynamics at the appropriate scale is crucial (Esch et al., 2014; Su, Xiao, & Zhang, 2012; Zhang & Seto, 2011). Practitioners have already recognised the strategic importance of developing technologies including remote sensing (e.g. FIG, 2010), to monitor urbanisation (Dewan & Yamaguchi, 2009; Haas, Furberg, & Ban, 2015; Kontgis et al., 2014), track changes of land cover and impervious surfaces (Castrence, Nong, Tran, Young, & Fox, 2014), inform strategies of urban planning in developing countries (Faour & Mhawej, 2014; Saksena et al., 2014). But how these techniques can help to map interactions between geology, subsurface resource exploitation (e.g. groundwater abstraction) and urban development at the surface still requires dedicated research.

In light of the limited and dated urban geographic literature

## 2. Materials and methods

### 2.1. Persistent Scatterer Interferometry (PSI)

PSI is based on multi-interferogram processing of long stacks of SAR images acquired from space-borne microwave sensors (at least 15–20 if collected on a monthly basis; tens if sampled with frequency of a few days), to extract the position of manmade objects on the ground and natural features such as outcrops, and reconstruct their displacements in time (Crosetto, Monserrat, Jungner, & Crippa, 2009). The output consists of sparse sets of points (Persistent Scatterers – PS) each of which is provided with a time series of LOS displacements vs. time, i.e. a plot where each dot is the displacement of the radar target as measured along the Line of Sight (LOS) of the satellite expressed in mm at the given date of acquisition (Tapete, Fanti, Cecchi, Petrangeli, & Casagli, 2012, 2015). Shorter repeat cycle of the satellite allows the retrieval of more dense time series. In the case of the ERS-1/2, ENVISAT and RADARSAT-1 sensors used in this research, consecutive displacement estimates are provided every 35 to 24 days.

These estimates are relative to a stable reference point which is physically positioned at a location the stability of which is assumed based on geological considerations or proved usually by means of GPS archive records. In the case at least 50 SAR images are

processed, the quantitative uncertainty ranges between  $\pm 2\text{--}5$  mm on single displacement estimate for each PS located less than 2 km from the reference point. Longer is the stack of images processed and more accurate are the displacement estimates. Although the sensitivity to detect small displacement varies from the near to the far range of the SAR image swath, this is negligible and it is commonly accepted that the sensitivity at the image centre applies to the whole swath of the image.

Within the resolution of the pixel cell, the PS barycentre is physically located in correspondence with highly backscattering objects or natural features that are coherent and maintain constant reflectivity properties throughout the acquisition period, so precise displacement measures are possible. This condition is a compulsory requisite for PS generation, that otherwise would be inhibited as it happens in vegetated areas or when the imaged scenario has significantly changed between two consecutive images.

Coordinates and elevation are provided for each PS. Recent research has proved the reliability of the PS geolocation for spatial attribution to buildings and portions of them (Tapete, Morelli, Fanti, & Casagli, 2015). In dense urban areas this is an important aspect to account for. The abundance and proximity of reflectors (urban targets are ideal radar backscatterers) result in high density of PS per square kilometre (from tens to thousands of PS/km<sup>2</sup>). This adds onto other important advantages offered by PSI compared to other techniques such as GPS and optical levelling, i.e. the availability of SAR data of medium resolution (25–30 m) since early 1990s (ERS-1/2), throughout 2000s (ENVISAT and RADARSAT-1/2) up to now, and wide area coverage with scene extent up to 100 km swath which is sufficient to provide a holistic coverage of large to megacities and metropolitan areas.

Of all the information associated to each PS, we use in this study the following two properties: (i) presence, meaning in this context whether the PS is permanently identified over an object on the ground or discontinuously during the time period of observation from space; and (ii) the displacement time series.

As proved in the above cited InSAR literature, data stacks acquired by different satellite sensors and/or from different orbits do not provide identical sets of PS, even when they are processed with the same InSAR algorithm and at equal conditions of spatial resolution, temporal coverage and image sampling frequency. Identified PS are indeed determined by the employed LOS geometry of acquisition and associated backscattering mechanisms.

## 2.2. Mapping of criticalities and rating methodology

Urban dynamics typically appear in PSI displacement maps as a cluster of moving PS (hereinafter referred as ‘pattern’) with extension and shape related to the nature of the detected phenomena (e.g. subsidence affects entire urban sectors, while consolidation of new foundation soils is limited to the area of recent construction).

To overcome the known PSI limitations (subjectivity of the interpretation, salt-and-pepper distribution of PS with associated velocity estimates affected by noise, presence of unrelated PS), we decompose each PS set into classes of velocity and display them in ‘Velocity decomposition maps’ (Fig. 1). PS with velocity values lower than a threshold  $V_{lim}$  are not displayed, as they are classified as stable objects.  $V_{lim}$  is established depending on the characteristics of the radar sensor, and in particular in relation to the minimum detectable displacement that is related to the employed wavelength. For the purpose of this study, the  $V_{lim}$  takes values of  $\pm 1.5$  mm/yr, in agreement with the wide InSAR literature (Colesanti & Wasowski, 2006; Righini, Pancioli, & Casagli, 2012).

Patterns (‘Alert areas’) are delineated at a mapping scale that depends not only on the resolution of the imagery, but also on the

size of the patterns themselves. In this paper, the mapping scale is up to 1:2500 (at larger scales micropatterns were found to be not easily recognisable).

Alert areas are classified using the terminology of ‘Macro-pattern’, ‘Micropattern’ and ‘Localised deformation’ proposed by Tapete and Cigna (2012a) and Tapete and Cigna (2012b), with some revisions to best represent the scale and shape of patterns associated to urban dynamics.

A Macropattern is defined as an Alert area extended over a region (typically a sector of the city) characterised by a concentration of moving PS compared to the rest of the area covered by the PS dataset and a lower density of stable PS. The motion is monodirectional and all the objects within the alert area show the same or nearly the same displacement trend, towards (uplift) or away (subsidence) the satellite along the LOS. Macropatterns generally correspond with widely extended phenomena. Examples are human-induced or natural subsidence, large landslides, compaction of soil in inland areas or in coastal land that has been recently reclaimed from the sea.

Micropatterns are drawn using the same rationale as macropatterns, but their extent is limited to single structures or small groups of buildings. Even though the specific intensity of the movement and the related consequences are generally higher than in Macropatterns, the deformation phenomena affecting points within a micropattern are typically due to local phenomena such as minor landslides, failure of retaining walls, tunnel excavations, settling of recent buildings, bridges or roads, sinkholes, imminent structural failures.

Isolated clusters of PS, generally referred to a portion of a structure, are categorized as Localised deformation and usually identify damages due to structural failures, degradation of non-structural elements (e.g. balconies), very localised ground instability. It is worth mentioning that the detection of localised deformation can be challenging and sometimes only solvable with ground truth validation, since individual PS can be generated by displacements of unrelated objects such as antennas or neighbouring light poles (cf. Pratesi, Tapete, Terenzi, Del Ventisette, & Moretti, 2015; Tapete & Cigna, 2012a).

PS classification indexes by Pratesi et al. (2015) are used to rate the structural health of individual buildings (Fig. 1). For each building, density and deformation rate of PS are converted into the classification indexes referred to as *Completeness of Information Index* ( $I_{ci}$ ) and *Conservation Criticality Indexes* ( $I_{cc}$ ), respectively. While  $I_{ci}$  is scored from A to E to indicate optimal to poor PS coverage over an individual building, a lower  $I_{cc}$  class indicates worse structural condition of the building.

In practice, once a pattern is identified in the velocity decomposition map, to downscale the assessment to the level of individual building, we intersect the polygon entries outlining the boundaries of the properties and their buffer with the PS falling within the pattern, and we extract  $I_{ci}$  and  $I_{cc}$  indexes. The downscaling is feasible and reliable when the degree of coverage of the PS over the property is sufficient (i.e.  $I_{ci}$  score from C to A).

## 2.3. Mapping of urban evolution

To the best of our knowledge, the InSAR literature has not investigated the systematic use of presence and absence of PS as numerical indicator of urban changes. The absence of measurement points is typically seen as a limitation of the InSAR techniques for purposes of deformation analysis (e.g. Bateson, Cigna, Boon, & Sowter, 2015; Cigna, Bateson, Jordan, & Dashwood, 2014a), while it is useful to spot on areas in urban settings that were not coherent during the period of observation, such as those under construction, demolition or renovation. These are modifications that significantly

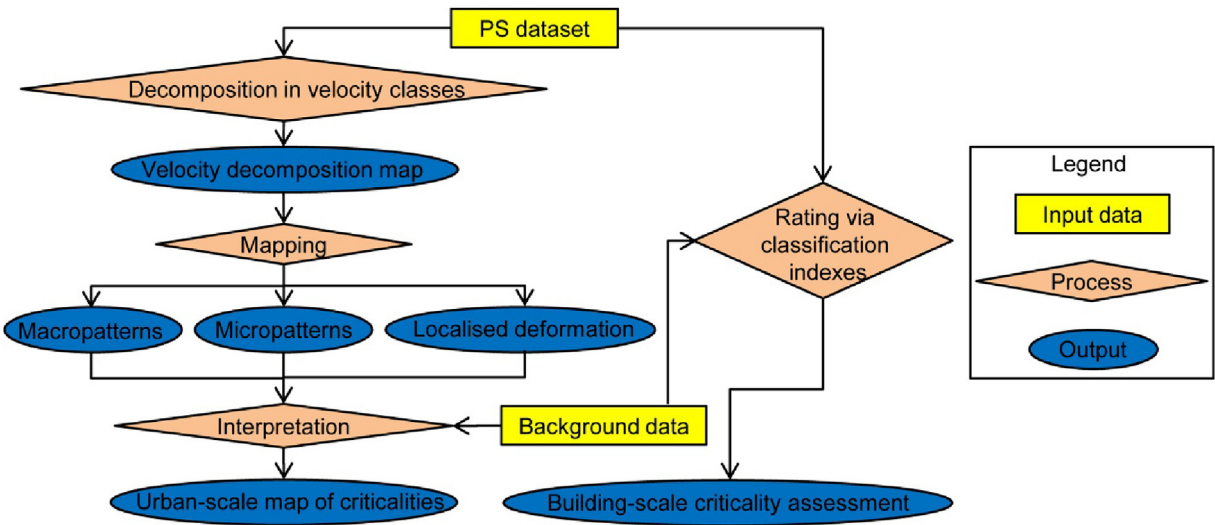


**Fig. 1.** Flowchart of the proposed PSI-based mapping methodology.

alter the local urban topography and geometry of the buildings and influence the persistence of radar targets within the scene imaged by satellite(s) in different periods and, consequently, control the likelihood of PS generation during the time series processing.

If we compare two maps showing PS spatial distributions  $PS_A$  and  $PS_B$  generated by processing SAR images acquired during the period A ( $PS_A$ ) and a later period B ( $PS_B$ ), respectively, the following situations can be found in those areas where significant alteration has occurred and the interferometric coherence as a requirement for PS generation has been modified:

- (i) increase of the number of radar backscatterers, i.e.  $PS_B > PS_A$ . Typical urban examples are: new construction; modification of pre-existing structures and buildings which, as a consequence, increase their radar backscattering properties; or land use change leading to an increase of backscattering surfaces (e.g. urban fabric, infrastructure).
- (ii) decrease of the number of radar backscatterers, i.e.  $PS_A > PS_B$ . In cities this is observed in areas of intentional demolition, collapses or land use change towards land cover with low interferometric coherence, such as from urban fabric to vegetation or bare soil.

With our method we are able to generate a "PSI-based map of urban evolution" (see Section 4.4, Fig. 5). Given the temporal frame of the SAR datasets commonly available over cities, this type of investigation consists of a comparison from a decade to the next one, as demonstrated later in section 4 with a change detection analysis from 1992 to 2000 to early 2000s–2010. In such circumstance the robustness and reliability of this method rely on the use of SAR images with similar resolution, acquisition geometry and parameters (including the incidence angle). For this reason, in this paper we combine ERS-1/2, ENVISAT and RADARSAT-1 Standard Beam PS datasets (see section 3.2; Table 1). This approach can be effectively applied to PS datasets of the same satellite with different temporal coverage, but this is outside the scope of this research.

PS are therefore used themselves to track horizontal transformations of the city and identify what sectors are developing and renovating or, at the opposite, are shrinking and decaying.

Our method can complement multi-temporal optical images, or even fill the lack of information when such imagery and orthophotos are not available or partially provide spatial or temporal coverage of the city. In this regard, the shorter repeat cycle with

which satellite SAR are acquired (monthly to a few days) compared to the typical orthophoto schedule (generally updated every one to a few years) is a further stimulus to attempt such use of PS.

### 3. Application on the urban area of Florence

#### 3.1. Test site and background information

The city of Florence is located in Tuscany region, central Italy, at about 50 m a.s.l., in the SE corner of NW-SE oriented elongated depression known as Florence-Pistoia plain (Fig. 2). With more than 370,000 inhabitants it is the eighth most populated Italian city, reaching over 1 million across the metropolitan area (ISTAT, 2014). For the purpose of this research we refer to the urban boundaries as shown in Fig. 2.

The urban growth of Florence started in Roman times (1st century BC), reclaiming land and expanding from the narrowest section of River Arno, which is still nowadays marked by the famous bridge Ponte Vecchio (Morelli, Battistini, & Catani, 2014). The most flourishing periods date back to Medieval (13–14th centuries BC) and Renaissance (15–16th centuries) Ages, with a complete urban re-organisation in 1860–1890s when the city became the capital of the new Italian State. In this period new infrastructure were constructed by cutting and reshaping the slopes of the surrounding hills, and residential quarters were built around the boundaries of the largely altered town centre.

Further expansion occurred westwards in 1950–1970s, during the post-WWII reconstruction and the so-called "Italian economic miracle". This phase of urban sprawl brought to a sort of peri-urbanisation where land cover is classifiable between agricultural, commercial and urban. In more recent time, this zone is subject to renovation. University Campus of Science was opened in the outskirt village of Sesto Fiorentino in early 2000s, while works are ongoing to prepare for the new tram transportation infrastructure and the planned development of the local airport Amerigo Vespucci. In this new era for the city of Florence, a key role will be played by the extensive tunnelling for the high-speed rail network (TAV; Mirri & Sargentini, 2005) that will run underneath a significant part of the urban area.

In such a challenging urban transition, the important elements to be accounted for to understand the interactions and feedbacks that can be triggered at urban to local scales include: the geological setting, the dense distribution and varied typologies of buildings

**Table 1**

Main characteristics of the PSI datasets used in this study. ERS-1/2 and RADARSAT-1 datasets were processed with PSInSAR™ technique according to Ferretti, Prati, and Rocca (2001), while ENVISAT with PSP-DIFSAR (Constantini, Iodice, Magnapane, & Pietranera, 2000).

Data stack	$\lambda$ [cm]	Orbit	Nominal repeat cycle [days]	Nominal resolution [m]	Time interval	N° SAR images	PS density over Florentine area [PS/km <sup>2</sup> ]
ERS-1/2 ENVISAT ASAR	5.66	Descending	35	25	24/04/1992 27/11/2000	79	172
	5.63	Ascending	35	30	16/10/2003 27/05/2010	35	400
		Descending			10/02/2003 28/06/2010	35	516
RADARSAT-1	5.6	Ascending	24	30	07/04/2003 28/10/2007	54	106
		Descending			25/03/2003 15/10/2007	47	98

with historical and architectural value. The latter span from traditional architecture to reinforced concrete and steel structures and are mostly officially included within the perimeter of the 505-ha UNESCO site inscribed in the World Heritage List since 1982 (Fig. 2).

From a geological point of view, the Florence-Pistoia plain is a structural basin that developed since Late Pliocene (Coli, Brugion, & Montini, 2013, and references therein) and was filled by fluvial-palustrine Plio-Pleistocene deposits. The latter were subsequently eroded by River Arno and its tributaries, to form a large valley at the bottom of which well-sorted gravel fluvial deposits accumulated. Further lateral erosion of the bedrock occurred in late Pleistocene, reaching the base of the southern hills (altitude up to 300–400 m a.s.l.), as well as the northern Plio-Pleistocene deposits, with a final phase of deposit accumulation in the Holocene. Therefore, most of the building environment lies over deposits of known susceptibility to subsidence, especially in the peripheral and suburban districts of the Florentine metropolitan area due to groundwater exploitation and load of new constructions (Canuti et al., 2005). Not less important are flooding hazard that periodically affected the city in centuries and caused several damages (Morelli et al., 2014), and ground instability in the hilly areas (e.g. Fanti, 2006). According to the official inventories, landslides are mainly classified as slow to very slow. This means that the effects on the overlying or neighbouring buildings and infrastructure may be seen after long time since the first movement of the landslide. Therefore only an analytical approach based on long temporal records such as PSI can enable the detection of the impacts of such slow landslides.

### 3.2. Input PSI datasets

Table 1 summarizes the PSI datasets used in this research.

Point shapefiles of PS were obtained by processing the full archives of C-band SAR accessed from the Canadian and European Space Agencies, with Persistent Scatterer algorithms. A simple linear model of phase variation was imposed during the processing and a false alarm rate equal to  $10^{-5}$  was applied.

A regular monthly frequency was achieved with ERS-1/2 and RADARSAT-1 datasets. The only exceptions are single limited gaps up to 3, 5 and 14 times the nominal repeat cycle. Despite the nominal 35-day repeat cycle of ENVISAT, both ascending and descending PSI datasets provide consecutive displacement estimates every 70 days.

30-m ray of surrounding areas and velocity thresholds were applied to account for the slight difference in spatial resolution and band length between the different data stacks (Pratesi et al., 2015). Deformation patterns and changes of the PS distribution were delineated by grouping the datasets as follows: ERS-1/2 descending PS for 1990s, ENVISAT and RADARSAT-1 PS for their overlapping coverage in early 2000s. Therefore two distinct scenarios were compared before and after year 2000 when Florence underwent an apparent urban transition (see section 3.1). Technically this approach is doable, given the similarities between the ENVISAT and RADARSAT-1 datasets, although wavelength and LOS differences

and the temporal shift between these two satellites result in different PS sets.

### 3.3. Sample of monuments for building-scale analysis

The downscaling has been carried out on a sample of monuments selected to be statistically representative of the variety of structural typologies and background conditions of the city (Fig. 2C).

We classified the structures into typology groups without considering ‘minor’ categories such as tabernacles and small churches, since the latter did not fit in the scale of the PSI data used in this research. Fig. 2C reports for each category the percentage over the entire population of the Florentine built environment and heritage.

## 4. Results and discussion

### 4.1. City-scale assessment

5 micropatterns and 5 macropatterns were detected based on ERS-1/2 descending (1992–2000) PS velocity decomposition map, while 12 macropatterns and 84 micropatterns by combining the ENVISAT and RADARSAT datasets (2003–2010). The increase in the number of patterns suggests that Florence experienced more changes in 2000s (Fig. 3), although it is to be noted that the higher PS density obtained from the more recent data enabled a clearer delineation of the alert areas.

The following background data and maps were used to attribute the displacement patterns: geology and morphology of the soil (Florence City Council, 2010; scale 1:10,000); presence of land movements and natural hazards (Florence City Council, 2010; scale 1:10,000); inventory of wells (Florence Province, 2014); cadastral maps (Tuscany Region, 2014; scale 1:10,000, and 1:2,000); land use (Florence City Council, 2015c; scale 1:10,000) and use of buildings.

Movements due to the settling of foundation soil are more evident in areas of fluvial deposits that are highly compactable and collapsible. Effects are observed where urban expansion recently happened, i.e. in the north-western part of the alluvial plain where all the new industrial and building construction activities concentrated. On the contrary, no major urban change or instability phenomena were observed within or near the UNESCO WHS which has been almost stable in the period of observation. This contrast matches with similar evidence found based on InSAR in other Italian historic cities in transformation such as Rome (Cigna et al., 2014b; Stramondo et al., 2008).

As expected, landsliding areas, one of which located south of the UNESCO boundaries in Monte alle Croci and Piazzale Michelangelo (Fig. 3C), occur where the morphology is hilly and the environment is more rural and less densely urbanised (e.g. polygons f and g).

With regard to the period 2003–2007, macropattern a (Fig. 3B and C) highlights a peripheral area of Florence affected by uplift as a surface effect of water rebound due to the reduction of industrial

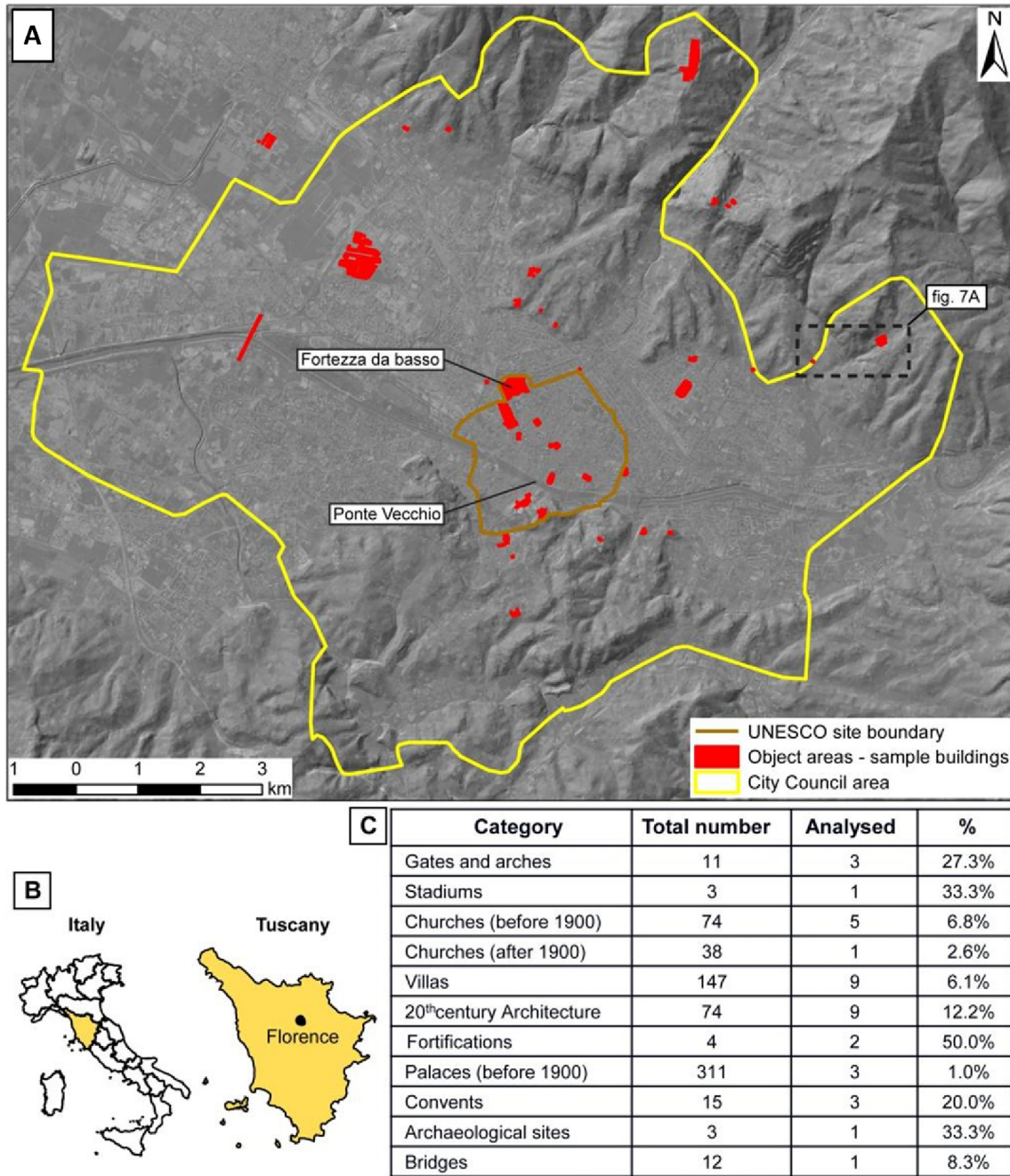


**Fig. 2.** (A) Map of Florence with indication of the study area corresponding with the Florence City Council territory (yellow region), the sample of selected monuments for building-scale analysis (red areas) and the boundary of the UNESCO site (orange line); (B) geographical location of Florence; (C) sample of the categories of heritage buildings analysed in this research. (For interpretation of the references to colour in this figure legend, the reader is referred to the web version of this article.)

activity and consequent decreased rate of groundwater abstraction. Conversely, the neighbouring macropattern b moving away from the satellite (Fig. 3B and C) corresponds with a storage area of alluvium, known as 'Area Mercafir'. The clear subsidence pattern (cf. also Fig. 8B) is likely due to a significant demand of groundwater from local aquifer to supply cooling systems. In both these areas no macropatterns were identified in the period 1992–2000 (Fig. 3A). This suggests that the movements likely started (or at least increased their velocity) after the year 2000.

Macropatterns c and e observed in the period 1992–2000 (Fig. 3A, C) partially overlap with macropattern d that refers to the period 2003–2007 in the south-west of Florence (Fig. 3B), an area

of relevant urban and industrial expansion especially during the last 20 years. The measured movements are mostly due to the settling of the foundation ground of recent structures, but with a clear temporal differentiation.

Areas covered only by macropatterns c and e were probably affected by building construction that diminished after 2000. As a consequence, the corresponding consolidation velocity decreased at an extent that no deformation were observed during the period 2003–2007. Conversely, buildings falling within the macropattern d only are more recent, with consolidation movements sensed exclusively after 2003.

The mutual intersections of macropatterns c with d and d with e

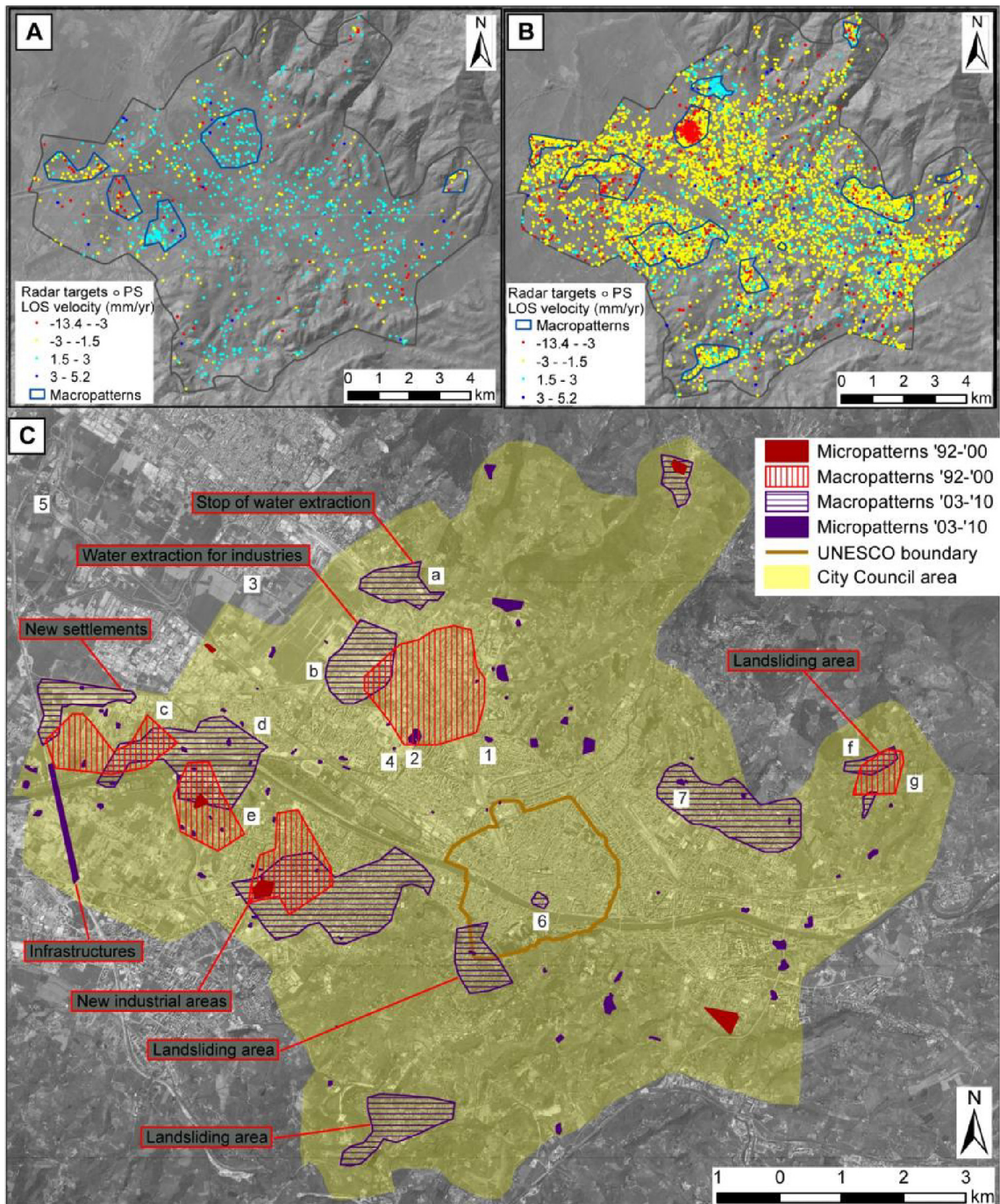


**Fig. 3.** Velocity decomposition map of (A) ERS-1/2 descending 1992–2000 and (B) ENVISAT descending 2003–2010, ENVISAT ascending 2003–2010, RADARSAT-1 descending 2003–2007, RADARSAT-1 ascending 2003–2007 and the respective macropatterns; (A) Map of alert areas of Florence with the indication of the analysed area (yellow region) and the boundary of the UNESCO site (orange line). (For interpretation of the references to colour in this figure legend, the reader is referred to the web version of this article.)

individuate areas where movements lasted from 1992 to 2010. This behaviour indicates a continuous building activity over this period with different timings for construction, but could be even explained by longer consolidation processes as a consequence of different properties of the soil and drainage systems. An exemplar of the complex dynamics picked up by PS datasets is offered later in the paper in section 4.3.2 (cf. Fig. 5).

Similar interpretation approach helps to unveil the already mentioned macropatterns f (referring to the period 2003–2007) and g (referring to the period 1992–2000) falling in a landsliding area north-east of the city centre (Fig. 3C). In this case the different

timing of observation of ERS-1/2 to ENVISAT and RADARSAT-1 captures the evolution of the geologic phenomenon as it was recorded from space before 2000 (area covered by macropattern g only), after 2003 (area covered by macropattern f only) and across the whole period 1992–2010 (area of overlap between the macropatterns f and g).

#### 4.2. Downscaling at single building scale

Classification indexes according to Pratesi et al. (2015) were calculated for the sample of 43 buildings reported in Fig. 2C.

The structural health of a building ( $I_{cc,o}$ ) is scored based on the PS maximum LOS velocity  $|V_{max}|$ , using the rating scale by which A means  $|V_{max}| \leq 1.5 \text{ mm/yr}$  and E  $|V_{max}| > 10 \text{ mm/yr}$ . Same scoring system applies to classify the structural stability of the area surrounding the building ( $I_{cc,a}$ ) by a buffer distance equal to the resolution of the SAR image (e.g. 30 m for ERS-1/2, ENVISAT and RADARSAT-1 PS datasets). The level of confidence with which these scores are provided is based on the amount of PS information available over the structure ( $I_{ci}$  score, from 'complete information' – Class A – to 'no data' – Class E).

**Table 2** summarizes the results obtained by classifying the ENVISAT ascending (2003–2010) dataset.

72.2% of the analysed buildings shows  $I_{cc,o}$  equal to A, meaning that a general stability is observed for the majority of the built environment. This figure matches with the overall stability of the historic centre that was observed at city scale via the velocity decomposition map and the resulting map of alert areas (see section 4.1).

Score D of  $I_{cc,o}$  is found in one situation only, i.e. the CNR complex which was built in early 2000s in Sesto Fiorentino, an area of land subsidence and settlement of new constructions (see full discussion in section 4.3.1 and 4.3.5; Figs. 4C and 8B).  $I_{ci}$  scored A confirms the highest degree of confidence possible associated with the assessment of the structural health of the building. In four situations D is the  $I_{cc,a}$  score of the areas surrounding the buildings of interest, meaning that wider patterns of ground instability affect the individual properties. No properties and their surrounding areas are classified E.

In addition to the CNR complex, other 7 buildings are classified with the highest degree of confidence, i.e.  $I_{ci}$  equal to A. Therefore only 18.6% of the total sample of 43 buildings shows a complete coverage of PS within the property boundaries; while in the majority of the cases (30 in total)  $I_{ci}$  is scored B or C. Complete absence of data is found in two circumstances only, i.e. Arco dei Lorena and Porta alla Croce, the former northern and eastern gates of the old Florence. In these situations no assessment of the structural health was possible and  $I_{cc,o}$  and  $I_{cc,a}$  could not be scored. Interestingly, the fact that this is found only in the case of buildings with limited planimetric extent proves that the spatial resolution of the ENVISAT images was sufficient to spatially resolve the majority of the urban fabric and heritage. So, apart from those two situations, the satellite resolution was not a limiting factor to carry out an accurate and reliable downscaling.

#### 4.3. Field validation and catalogue of urban dynamics

Based on the above results and the evidence that only a few buildings were scored in the worst classes (from C to D) and

**Table 2**

Distribution of classification indexes over the sample of 43 structures calculated by means of the PS-based rating procedure. The data are referred to the ENVISAT ascending PS dataset. Notation:  $I_{ci}$  – Completeness of Information Index;  $I_{cc,o}$  and  $I_{cc,a}$  – Conservation Criticality Indexes for the object and its surrounding area, respectively.

	$I_{ci}$	$I_{cc,o}$	$I_{cc,a}$
A	8	26	24
B	15	5	4
C	15	4	7
D	3	1	4
E	2	0	0
Total	43	36	39
% A	18.6	72.2	61.5
D + E	5	1	4
% D + E	11.6	2.8	10.3

therefore needed a deeper investigation, we inspected 19 structures, i.e. 44.2% of the selected sample, to correlate alert areas and classification indexes with ground truth.

A catalogue of urban dynamics has been found in Florence and exemplars are provided with regard to:

- consolidation of newly constructed buildings (section 4.3.1)
- evolution of the built environment (section 4.3.2)
- urban sectors with structural damages (section 4.3.3)
- slope and unstable areas (section 4.3.4)
- land subsidence (section 4.3.5)
- heritage buildings (section 4.3.6)
- condition assessment prior to underground excavations and tunnelling (section 4.3.7)

The ground truth reported in the following sections is based on visual inspections. When possible owing to data accessibility, the PS displacement estimates were validated with contemporary archive field measurements (e.g. water-well data in section 4.3.5). No new in-situ measurements such as GPS measurements were carried out. This is always recommended when the mapping of urban dynamics is based on PS data obtained from processing of recently acquired SAR images.

##### 4.3.1. Consolidation processes of newly constructed buildings

Soil compaction is an intrinsic consequence of the ground overloading due to new structures (Terzaghi & Peck, 1967). The entity of lowering depends on: the foundation typology, the mass of the building, the ground compressibility and the hydraulic condition of the soil. As soon as the building construction is complete and the load applies, the typical displacement trend consists in a first period of high deformation velocities soon followed by a strong deceleration that leads to stability after years. Considering the order of magnitude of compaction velocities, typically few millimetres per year, PSI offers an optimal sensitivity to observe such phenomena.

The examples shown in Fig. 4 refer to three types of urbanisation effectively enhanced by the map of alert areas of Florence: (i) new buildings and commercial complexes as result of a renovation project in an urban area of previous long-standing urban settlement; (ii) new urban sectors replacing ex industrial areas; (iii) urban expansion in out-of-town areas.

The new complex of piazza Leopoldo (label 1 in Fig. 3C) replaced an ex industrial estate left in the 1980s inside an area saturated during the first half of the 20th century. Between 2000 and early 2003 underground parking space, two residential buildings at north-east and south-east corners and a supermarket along the west side were built. The PS shown in Fig. 4A depict the period of soil consolidation after the construction completion. The time series confirms that the building subsided with the typical shape of the curve due to soil compaction caused by the overloading, with a sharp slope of the LOS displacement velocities recorded during the first year.

The urban sector between via di Novoli and viale Guidoni (label 2 in Fig. 3C) is an example of large industrial areas completely renovated to respond to the space needs of the growing city. The FIAT car factory was demolished at the end of the 1990s and the cleared site was used to host the headquarters of a bank, the new Palace of Justice of Florence, the University faculties of Law and Social Sciences, the Hilton hotel, a commercial centre and a 32-ha green area, with major building activities carried out between 2000 and 2008. The PS displacement map in Fig. 4B reflects these changes during the acquisition period 2003–2010. Buildings finished before 2003 are experiencing subsidence due to soil compaction, old industrial buildings left for museum purposes

appear stable, buildings realised after 2003 are not covered by measurement points due to lack of coherence and consequent constraint to generate PS. The PS labelled b1 in Fig. 4B refers to the Palace of Justice whose structures were finished at the beginning of 2003 when ENVISAT satellite started recording radar images of the area. The displacement trend, with a considerable deceleration at the beginning of the acquisition period, is typical of soil compaction dynamics. The same behaviour characterises the PS labelled b2 in Fig. 4B which refers to the underground parking of the hotel.

The new headquarters of CNR (National Research Council) (label 3 in Fig. 3C) was completed at the beginning of the 21st century and is located in a plain lying between the north-western suburbs of Florence and the neighbouring borough of Sesto Fiorentino (Fig. 4C). This land was reclaimed from marshes since the 1930s and became a peri-urban area with patchwork development and mixed land use, including pasture. The CNR complex consists of six buildings built progressively starting from the southern side. This clearly appears in the PS displacement map in Fig. 4C where southern buildings started to settle before the others and therefore show higher displacements than the northern ones. Time series c1 and c2 (Fig. 4C), relative to more recent and older buildings respectively, differ not only in the total cumulative displacement (6 cm against 1 cm), but even in the non-linearity of the trend of soil compaction.

In this regard it is worth noting that non-linear trends are observed in some of the time series and frequently manifest as seasonal variations due to thermal expansion of the structures. Nonetheless, as seen in Fig. 4C, in most of the cases the time series are dominated by subsidence motion. Therefore, while the trend is not linear and is the result of a mixture of movements, there is no doubt that the structures have subsided during the period of observation. As recently discussed in Pratesi et al. (2015), this type of trend is found in other areas of the city, including green spaces. There the seasonality was due to the natural response of shrink-swelling soil.

#### 4.3.2. Evolution of the built environment

Fig. 5A and B shows the above discussed ex-industrial area of piazza Leopoldo (label 1 in Fig. 3C). As proved by the 1999 orthophoto (Fig. 5A), the area was abandoned before the renovation work started, partially covered by vegetation and ruins were partially removed. This condition is seen as absence of PS in the ERS-1/2 PS displacement map (1992–2000). On the contrary, the ENVISAT PS displacement map (2003–2010) shows PS over the new buildings indicating that no further perturbation occurred there during the acquisition period. Therefore this example falls within the case (i), i.e.  $PS_B > PS_A$  categorized in section 2.3.

The opposite situation happens when demolitions have occurred (case (ii),  $PS_A > PS_B$ ). In the area along Viale Belfiore (cf. label 4 in Fig. 3C) an industrial estate was demolished in late 2005 – early 2006. The construction works started quite soon after and were completed in 2014. This sequence is correctly captured in Fig. 5C and D that report the PS displacement map from ERS (1992–2000) and ENVISAT (2003–2010) data, respectively. While the older data provide a homogeneously dense distribution of PS covering the roof of the former building, no PS are retrieved for the first decade of 2000s due to the demolition and reconstruction activities.

Therefore, evolution of the built environment can be tracked based on presence/absence of PS data only.

#### 4.3.3. Urban sectors with structural damages

Guided by the map of alert areas we concentrated on micro-patterns which appeared as 'unstable islands' within rather stable quarters. In situ checks were undertaken in the micropattern (cf.

label 7 in Fig. 3C) drawn in the north-west of Florence between Cocchi, Fibonacci and Baldesi streets (Fig. 6). Multi-sensor PS data, especially along descending orbits, indicate movements extended over the whole blocks of buildings in the first decade of 2000s. Field surveys revealed the presence of damaged buildings, fissures on pavements and cracked walls, even in correspondence with the heritage building of the Agronomic Institute built in 1904 (south-east corner in Fig. 6). Interestingly, background data, including geological and geomorphological maps (Florence City Council, 2010; scale 1:10,000) do not report natural features predisposing to instability such as contacts between different geological units, mapped landslides and slopes. Although in this circumstance no other information was found to explain these motions, this real-world case study is an exemplar of what the proposed method can offer to allow the detection of ongoing processes occurring in areas that are not officially recognised as prone to instability, or of which no other evidence may have otherwise been retrieved.

#### 4.3.4. Slope and unstable areas

In Florence foundations of manmade structures were sometimes positioned in slopes affected by ground motions, so as to require mitigation measures via restraint works and dedicated systems of surface water management (Fanti, 2006). Some of the slope alert areas do not match with records of active landslides officially mapped in landslide inventories. In such circumstances, the detection of motions based on PS data can be of great benefit, pending confirmation from in situ inspections.

Fig. 7A shows one of these areas, located near the eastern boundaries of the City Council (cf. labels f and g in Fig. 3C). We focus here on the following two structures: a private country house near River Mensola (Fig. 7B) and the public cemetery of Settignano (Fig. 7C) in correspondence of which quiescent landslides are mapped in the official landslide inventory of Tuscany region (Tuscany Region, 2006; scale 1:10,000).

The movements of the country house revealed by PS would not have been detected based on visual evidence of damages over the exterior surfaces because of the recent maintenance works. Sealing effect is among the constraints which need to be accounted for during inspections in urban and residential areas, as they can limit ground truth collection. On the other hand, many signs of ground motions were found nearby, including cracks on the retaining walls (detail b2 in Fig. 7) and serious damages to the road which was closed for restoration works in correspondence with the bridge on River Mensola. Soil susceptibility is even confirmed by the geomorphological map of Florence (Fig. 7B) where different forms of instability are mapped not far away from the building.

The slope along which Settignano cemetery is located (Fig. 7c1) was reshaped in the last century with artificial materials. During field inspections minor damages were observed on the pavements and tombs, while major damage indicators were seen on service buildings (Fig. 7c2) and some chapels (Fig. 7c3). Unstable PS are likely due to both localised compaction of the embankments and more extended land surface processes. Indeed the cemetery lies on a quiescent landslide in the official landslide inventory of Tuscany region (Fig. 7A), while active land movements are mapped in the geomorphological map of Florence City Council (Fig. 7C).

#### 4.3.5. Land subsidence areas

In the case of plains intensively urbanised, groundwater extraction is the most common causative factor of land subsidence. In this regard, the Florentine alluvial plain extended until Prato and Pistoia is a demonstrative case study, as it was occupied during the last 50 years by industrial activities that massively exploited local aquifers.

The land subsidence is estimated with PS as accurately as

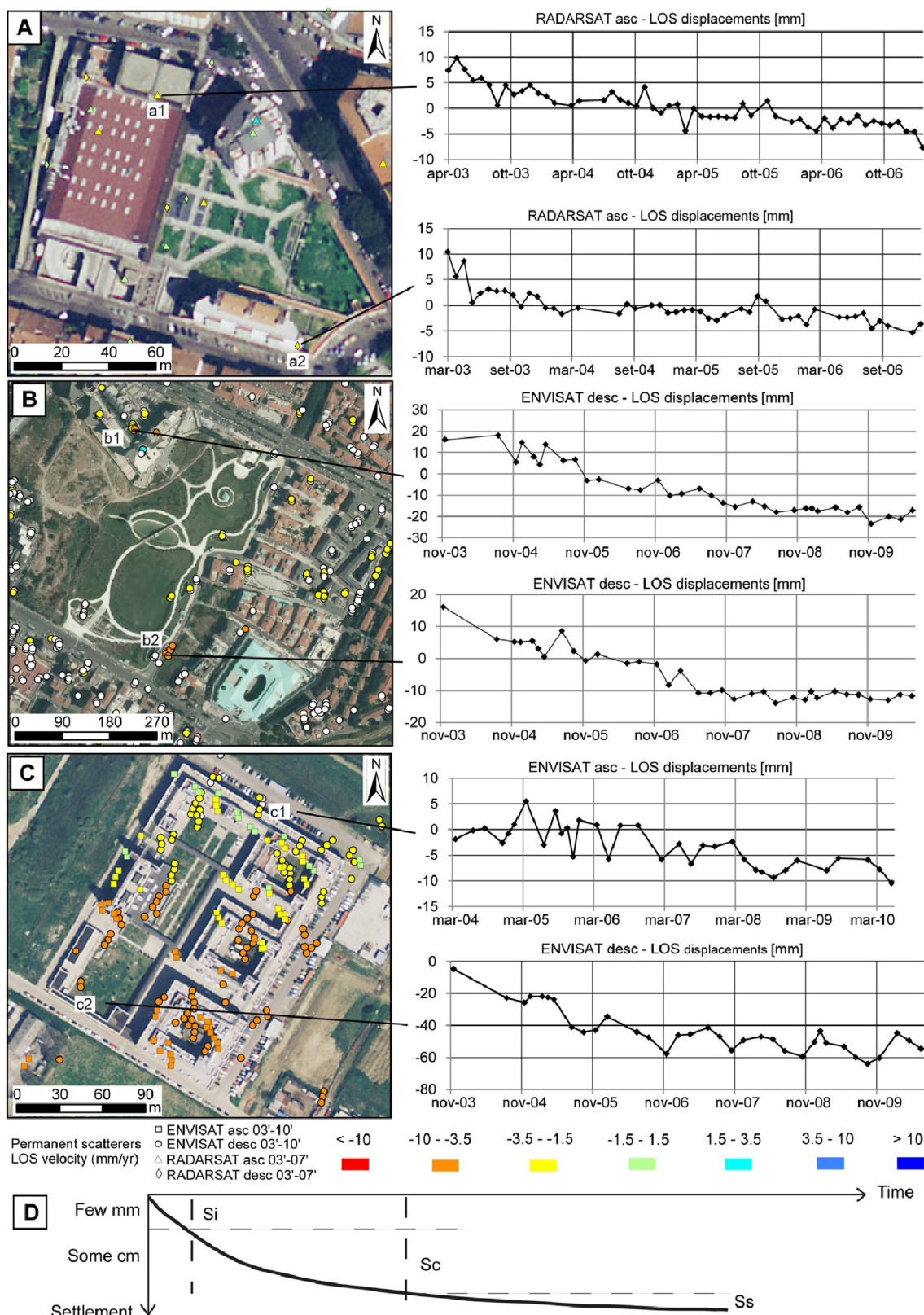


**Fig. 4.** PS displacement maps and time series of buildings showing consolidation processes: (A) piazza Leopoldo commercial and residential centre; (B) the area of urban renovation between via di Novoli and viale Guidoni. (C) CNR complex in the Council area of Sesto Fiorentino. (D) Theoretical curve of settlement induced by urbanisation. Si: settlement during construction; Sc: primary consolidation process; Ss: secondary consolidation process (modified from [Stramondo et al., 2008](#)).

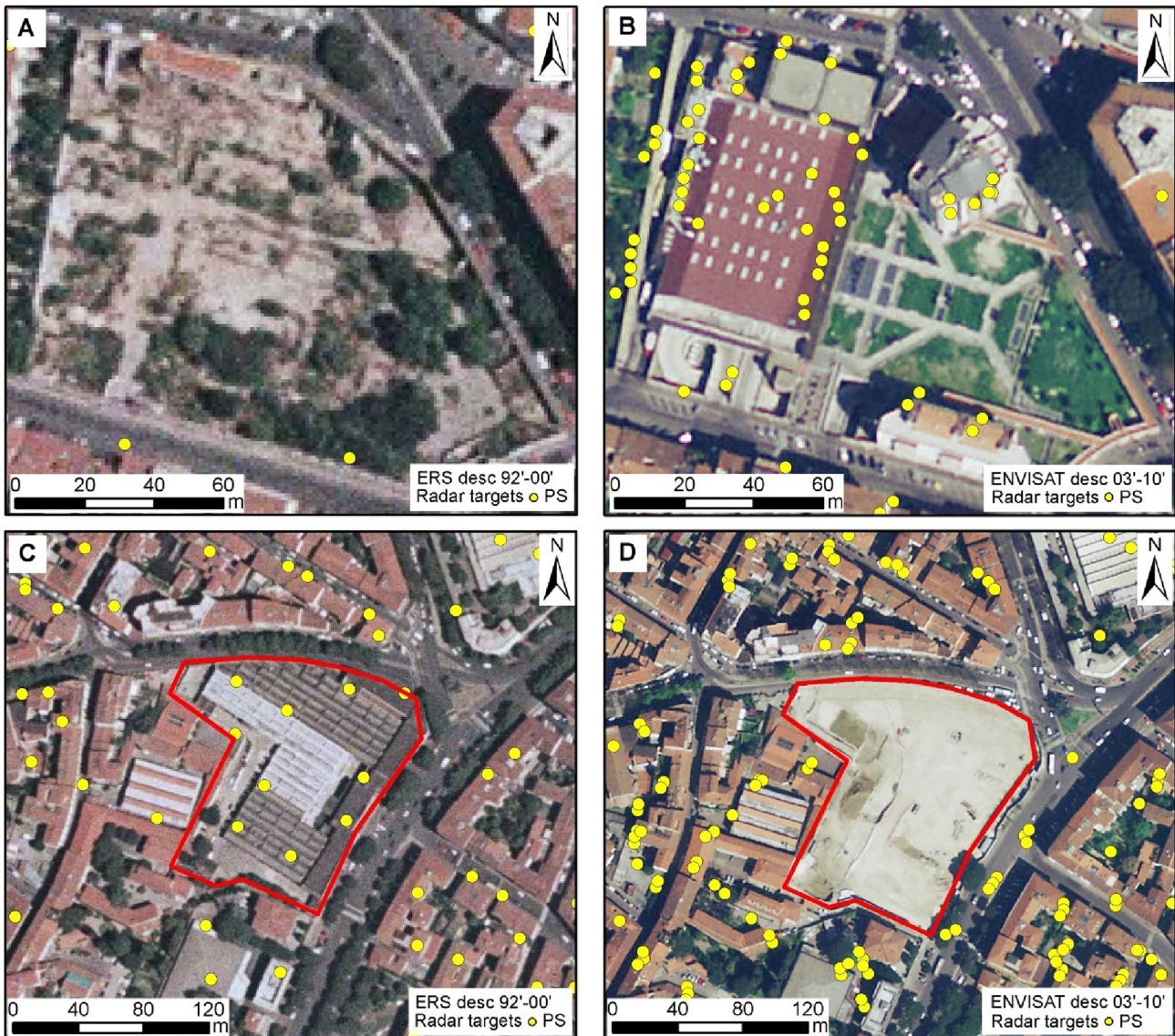


**Fig. 5.** PS evidence of the newly constructed commercial and residential centre in piazza Leopoldo by comparing: (A) ERS-1/2 descending 1992–2000 PS onto 1999 orthophoto; and (B) ENVISAT descending 2003–2010 PS onto 2006 orthophoto. Effect on PS generation due to demolitions in the transforming area along viale Belfiore (red contour) as observed from: (C) ERS-1/2 descending 1992–2000 PS displayed over a 1999 orthophoto; to (D) ENVISAT descending 2003–2010 PS displayed over a 2006 orthophoto. PS data are intentionally displayed without a colour scale of classification by LOS velocities. (For interpretation of the references to colour in this figure legend, the reader is referred to the web version of this article.)

±3 mm on single displacement estimate. Interpolated LOS displacement velocities were interpreted against the distribution and type of the wells as per the official inventory sourced from Florence Province ([Florence Province, 2014](#)). This database provides single measurements of the water table depth in the years 1970, 1971, 1997, 2002, 2007, 2008, 2010, but these records are pointwise, discontinuous and not available for all the wells. Therefore our analysis accounted for the constraints due to this lack of information. Nonetheless, it is clear that the most severe subsidence patterns in the valley coincide with sectors of intense recent urbanisation and management of factories storing and supplying goods.

Uplift affecting Sector 1 in [Fig. 8](#) relates to an industrial area where water pumping diminished since 2000 as a consequence of the economic crisis (cf. [Lu, Casagli, & Catani, 2010](#)). The water rebound, that is causing groundwater flooding of underground structures such as parking space and cellars, is likely the cause of

local ground uplift. Public media and dedicated workshops recently contributed to raise the attention and confirmed the societal impact of this phenomenon.

Sector 2 in [Fig. 8](#) is an industrial district in the municipal area of Calenzano, where a considerable number of wells is mapped. However, displacement measured using ENVISAT images are not of particular concern, especially in the northern part of the sector, where the depth of compressible soils is lower ([Pranzini, 2008](#), [Fig. 1](#)). It is also to be noted that a large portion (59.3%) of the wells serve domestic dwellings, therefore their incidence on total amount of groundwater abstracted is limited.

In sector 3 shown in [Fig. 8](#), i.e. the industrial district known as Osmannoro, a clear correlation is found between industrial activities, mapped wells and measured displacements. Comparison with the satellite optical imagery and orthophotos available since early 2000s evidences that this area did not change in the last fifteen years, thus confirming that the observed subsidence is the surface

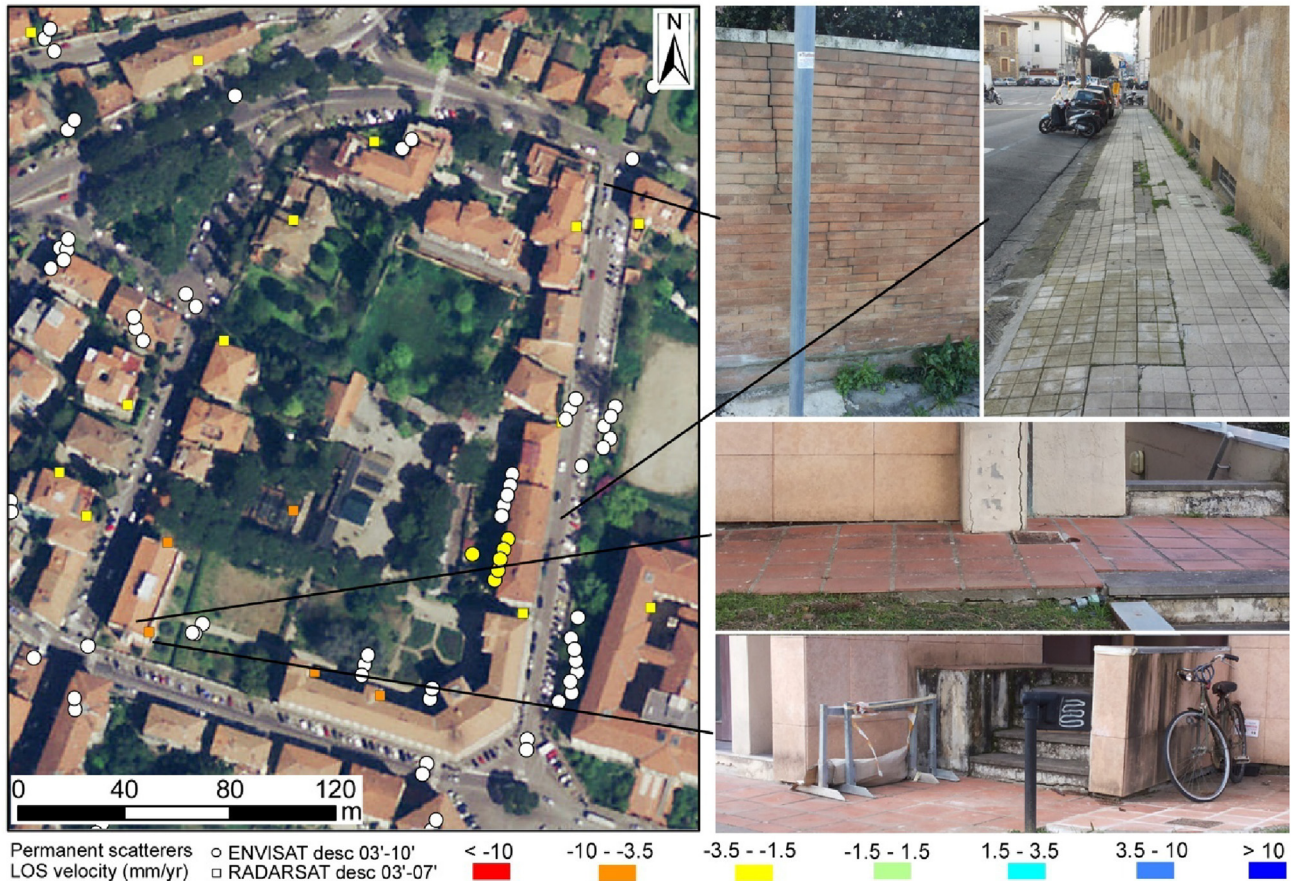


**Fig. 6.** ENVISAT descending 2003–2010 and RADARSAT descending 2003–2010 PS displacement maps of the block of houses and offices located between Baldesi (left), Cocchi (bottom) and Fibonacci (right) streets. Zoomed pictures show the damages observed on the buildings, walls and pedestrian pathway.

effect of groundwater exploitation.

The same cannot be stated for the area of CNR buildings (see Fig. 4C and centre of Fig. 8A and B), despite the same geological setting and the similar order of magnitude of LOS displacements away from the satellite. As commented in section 4.3.1, this is a clear case of settling of new buildings due to soil compaction.

Although very helpful, the information provided by wells is not always fully explanatory of the deformation patterns observed. An example is the Mercatir area, i.e. the major commercial centre in Florence for distribution of fruits and vegetables, hosting several storage buildings with a high demand of water for refrigerators. The presence of a lowering macropattern is then reasonably justified by the intense water pumping activity, although such correlation is not particularly enhanced by the official inventory of wells (Fig. 8).

#### 4.3.6. Heritage buildings

Three case studies with different typology, extension and age of the monuments and distinct deterioration process are described: (i) a complex and large monument with evidence of local damages; (ii) a medium-size, isolated and modern structure; (iii) an entire urban sector.

Forteza da Basso, a fortress dating back to the 15th century, is located in a crucial sector of the city, between the historic centre and the 19th–20th century expansion area (cf. Fig. 2A). The area is surrounded by the principal communication lines and is dense of important works concerning the ongoing urban renovation, including the underground parking realised in 2003–2005, the underground by-pass excavated in 2003 and the future tunnelling for the high speed trains (Figs. 9A and 10D).

In this urban context, the key added value of looking retrospectively at the recent surface deformation is twofold: diagnose the health of the historic asset and identify potential structural weaknesses which could be exacerbated by stresses due to the planned infrastructural works.

ENVISAT (2003–2010) displacement maps indicate some movements, especially in the northern portions of the walls (Fig. 9A). Those displacements, previously observed and classified by Tapete and Cigna (2012a), are located along the wall edge in the northern and north-western bastions facing the area where the underground parking was realised from 2003 to the end of 2005. In situ checks have confirmed the existence of damage in correspondence of the individuated displacements (Fig. 9A). The PS time series show somewhat non-linearity of LOS displacements. Deformation was recorded starting from 2007 in the PS located over the northern bastion and earlier in those over the north-western one. In absence of independent instrumental measurements simultaneous to the excavation works, more detailed investigations would be required to understand whether there was an impact on the stability of the bastions. In terms of geological factors, the underlying lithology, typical of alluvial plains, is uniform and no sources of soil instability are mapped. Nonetheless, such localised deformation is an important piece of evidence about the differential structural condition of the fortress to be aware of, in the perspective of future monitoring or prioritization of restoration and consolidation works.

The classification indexes calculated for the fortress as a whole monument according to Pratesi et al. (2015) are quite informative. In the period 1992–2000 both the architectural complex and the

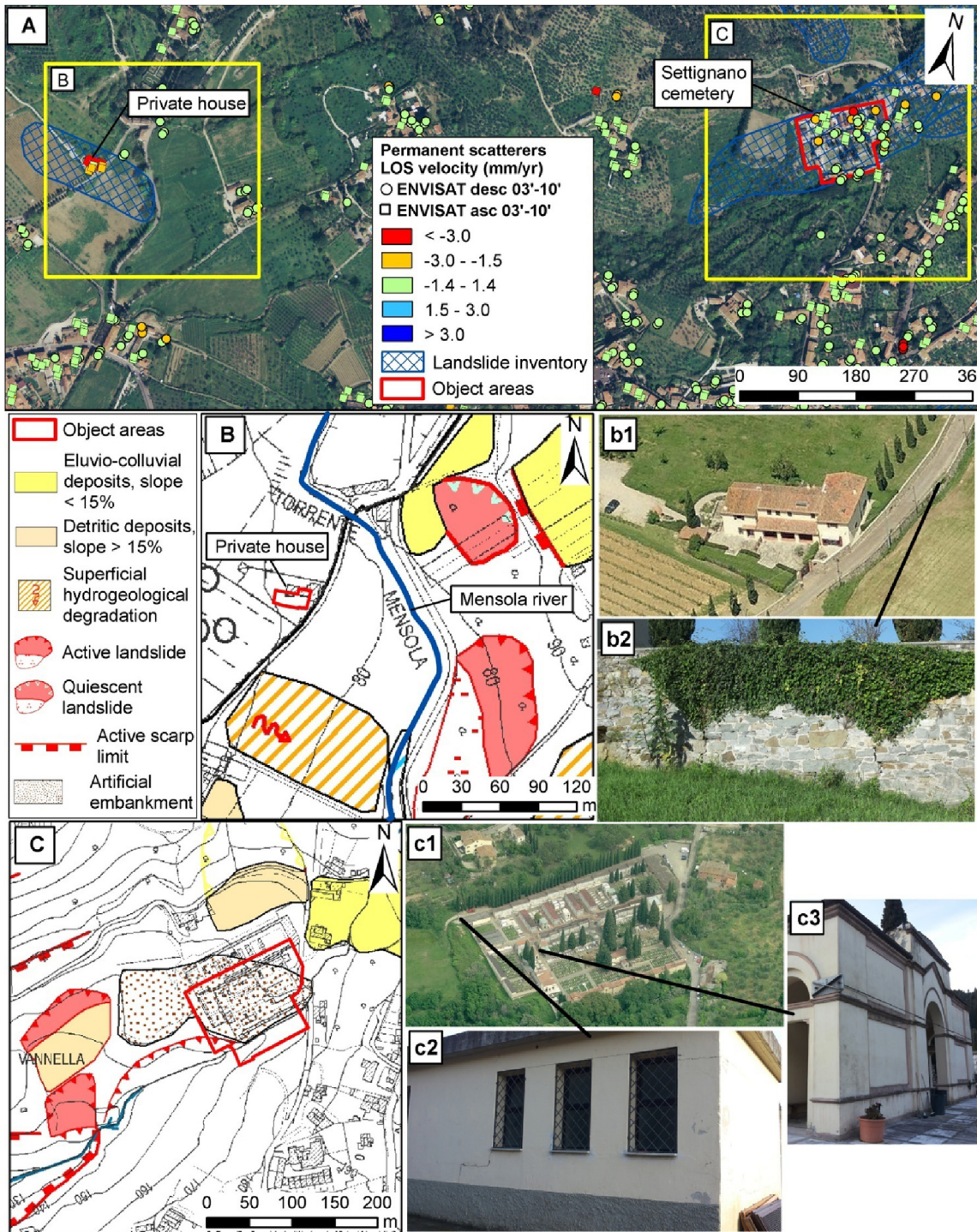


**Fig. 7.** (A) ENVISAT descending and ascending 2003–2010 PS onto the orthophoto of the area indicated in Fig. 2 and the official landslide inventory of Tuscany region; (B) detail of the geomorphological map of Florence City Council (modified from [Florence City Council, 2010](#)) in the area of the private country house near River Mensola (b1) (© BingMaps) and photo of wall fissures (b2); (C) detail of the geomorphological map of Florence City Council (modified from [Florence City Council, 2010](#)) in the area of the Settignano cemetery (c1) (© BingMaps), fissures on a storage building (c2) and consolidation works of an ancient chapel (c3).

surrounding areas were classified as stable with  $I_{cc,o}$  and  $I_{cc,a}$  equal to A, while the localised deformation observed in 2003–2010 result in worse score up to C.

San Giovanni Battista church is one of the most important pieces of modern architecture in Florence. It was designed by the engineer Pier Luigi Nervi and built between 1962 and 1964 outside the city, at the junction of two motorways (label 5 in Fig. 3C). The

movements evidenced by ERS descending and ENVISAT descending PS displacement maps can be associated to the state of conservation of some of the concrete structures as observed during the field inspection (Fig. 9B). Score D for  $I_{cc,o}$  of ERS descending data needs consideration and further investigation might inform future decisions for restoration works.

As already commented in section 4.1, the historical centre of

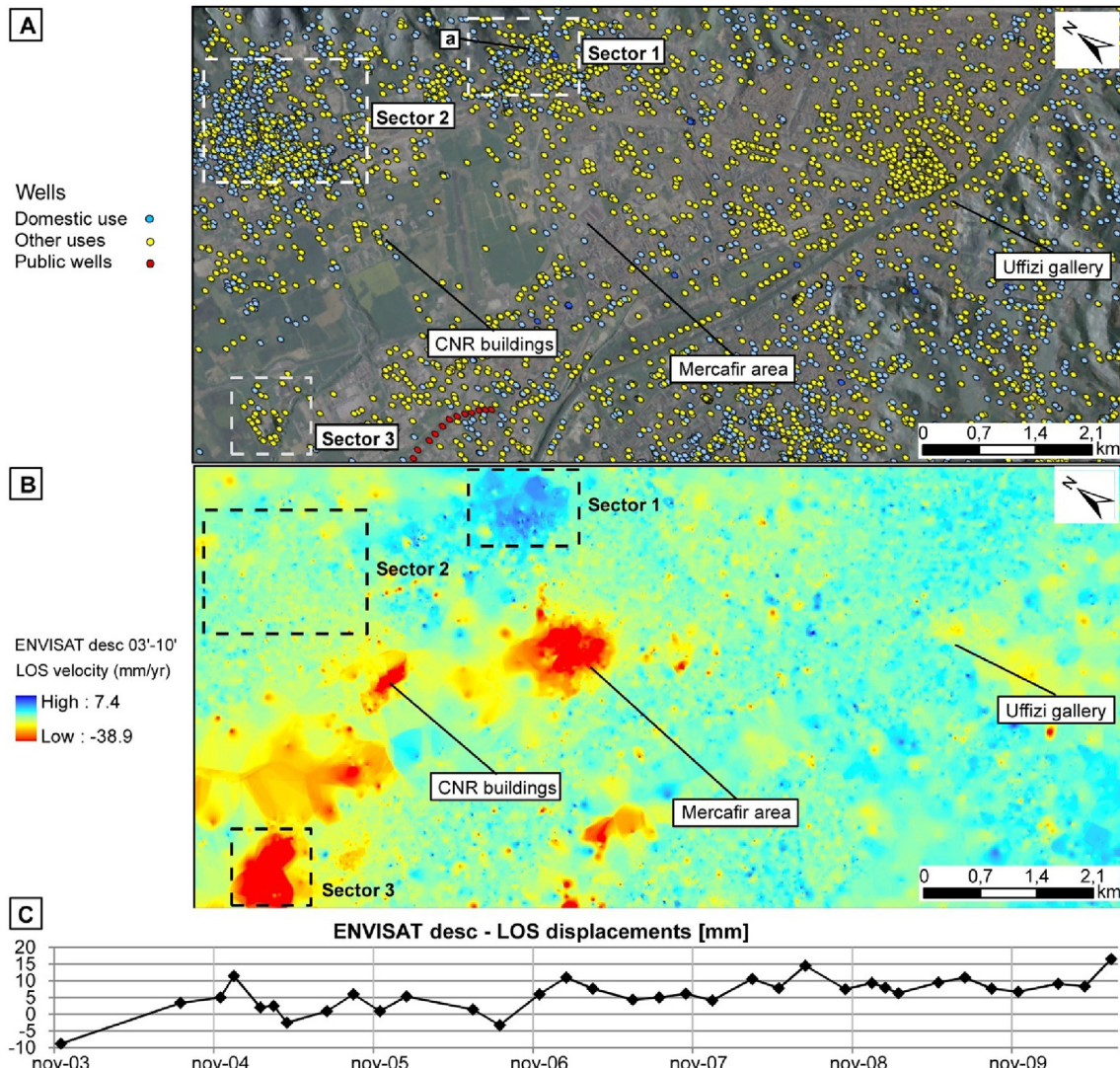


**Fig. 8.** (A) Official inventory of wells (Florence Province, 2014). (B) IDW interpolation of ENVISAT descending 2003–2010 PS, both displayed on DTM hillshade (10 m resolution). (C) Velocity plot of PS (a) in box A as an exemplar of the uplift trend observed within the time series.

Florence is the most stable sector of the city. The only exception is the area shown in Fig. 9C and D, where a significant number of the Florentine cultural heritage assets concentrate, including the Uffizi Gallery, Ponte Vecchio and Piazza della Signoria. A macropattern was here drawn to account for the diffused movements observed in the ENVISAT descending PS displacement map (see Fig. 3C, label 6).  $I_{cc,o}$  and  $I_{cc,a}$  are both scored C over the Uffizi Gallery. Up to date, neither significant restoration nor consolidation works were necessary to preserve the monuments, nor damage evidences were found during field surveys or were reported in official documentation. No discontinuities or peculiarities characterise the local geology and geomorphology of the area, which is homogeneous over the entire city centre. The nature of the macropattern is not easy to define, even considering the difference between velocity values of the ENVISAT ascending (Fig. 9C) and descending (Fig. 9D) displacement maps. One of the hypotheses recently proposed by the local geological community would suggest groundwater pumping to supply air conditioning system as the cause of soil compaction (pers. comm.). The high density of offices and stores in the area, coupled with the considerable amount of wells officially declared to the authorities (see Fig. 8A), might explain the expected seasonal variation of local groundwater level. Although further

investigations are required, this is a clear example of PS capability to enhance hot spot areas as 'isolated islands' of movement and deformation within stable urban sectors.

#### 4.3.7. Condition assessment prior to underground excavations and tunnelling

Previous experience with InSAR in cities like Milan (Colesanti, Ferretti, Prati, & Rocca, 2001), Naples (Terranova et al., 2015), London (Cigna et al., 2014a) and Shanghai (Perissin, Wangb, & Lin, 2012) demonstrates that PS monitoring can be a doable solution to assess and potentially forecast the impact of new infrastructure.

Figs. 9A and 10D show the planned track of the new underground railway for high speed trains (Florence City Council, 2015a) which will run in proximity to monuments like Fortezza da Basso and the ancient gates of Piazza della Libertà (Fig. 11A).

Moving across Fig. 10 from east to west, the first building to mention is Palazzo Mazzoni, designed by the futurist and rationalist architect Angiolo Mazzoni. This building was constructed in 1930s as part of the dwellings of the State railway company (Fig. 10A). Based on ENVISAT ascending (2003–2010) PS data (Fig. 10B), the building is scored with  $I_{cc,o}$  and  $I_{cc,a}$  equal to A, and its condition does not raise any concern. This is also suggested by ENVISAT

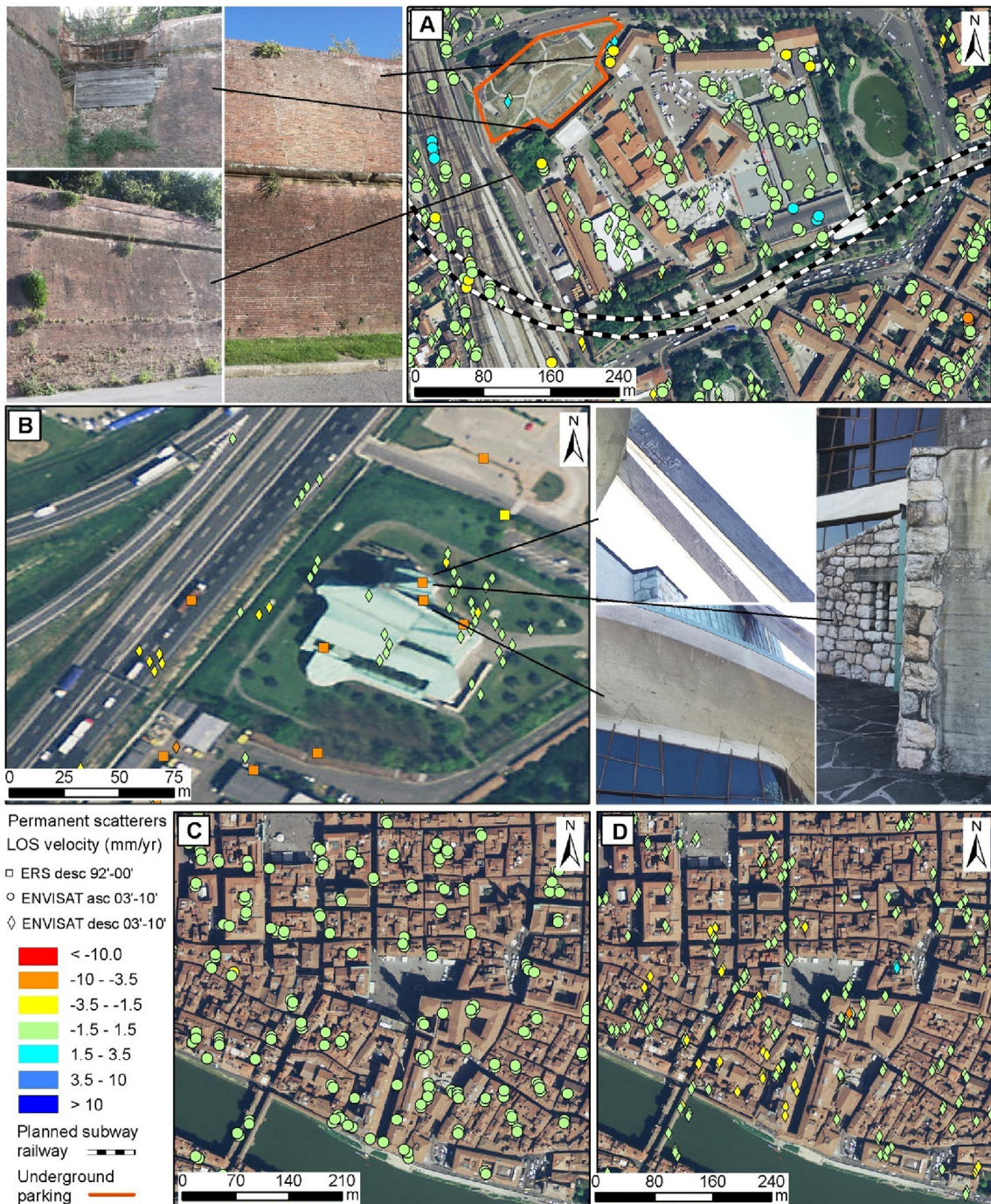


**Fig. 9.** ENVISAT descending 2003–2010, ENVISAT ascending 2003–2010 and ERS descending 1992–2000 PS displacement maps and damage evidences; (A) Fortezza da Basso complex with location of the underground parking (red polygon); (B) Chiesa di San Giovanni Battista; (C) and (D) the area around Uffizi Gallery. (For interpretation of the references to colour in this figure legend, the reader is referred to the web version of this article.)

descending and both RADARSAT-1 geometries in the first decade of 2000s. Given the historical and architectural value of this building and its current stable condition, particular attention should be paid in future PSI monitoring to assess whether the planned excavations can cause structural damages. Further element to think about relates to the impact of the new tramway system called Tramvia. The planned Line 2 is designed to pass through a tunnel coming out from the southern façade of Palazzo Mazzoni (Florence City Council, 2015b; Toc Toc Firenze, 2015, Fig. 10C). Estimates of the deformation occurred in 2003–2010 will act as a baseline

characterisation against which future InSAR measures may be compared.

Similar consideration can be done for the residential buildings and offices dating back to the 19th century, located along Viale Spartaco Lavagnini (Fig. 10D), underneath which the underground high speed subway will run.

According to the ENVISAT ascending PS dataset, Porta San Gallo, one of the remaining gates of the medieval Florentine city walls, appears to be almost stable during the period 2003–2010 ( $I_{cc,o}$  and  $I_{cc,a}$  equal to A). The absence of PS coverage in ERS descending

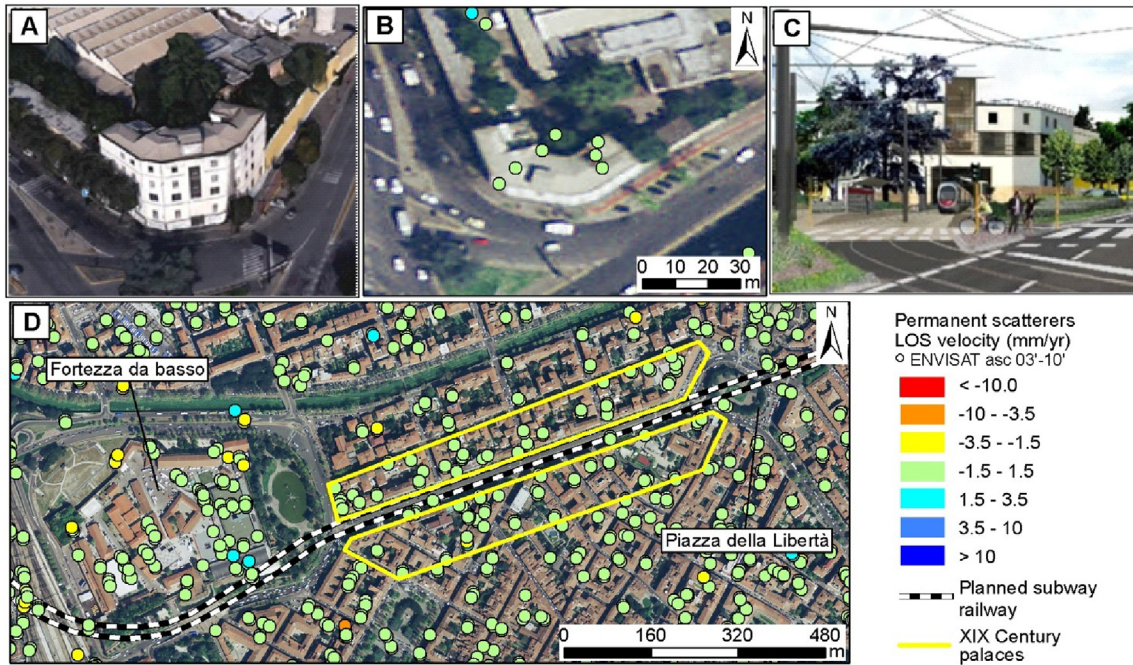


**Fig. 10.** Palazzo Mazzoni: Aerial view (A) (<sup>©</sup> GoogleEarth), (B) ENVISAT ascending 2003–2010 PS and (C) rendered external view showing how the building will look like once the new tramway system is constructed. (D) Area of viale Spartaco Lavagnini, with indication of the 19<sup>th</sup>–20<sup>th</sup> century buildings that might be of interest in relation to the new underground railway track according to Mirri and Sargentini (2005).

(1992–2000) does not provide information to confirm the same condition during the previous years (Fig. 11A).

Differently, ERS descending  $I_{cc,a}$  equal to A gives some elements to suppose the absence of criticalities during the period 1992–2000 for the 19th century Lorena triumphal arch. This monument, located just in front of Porta San Gallo (Fig. 11A), was repeatedly restored during the last 20 years. The superficial degradation that

was visible until recent times was likely due to the intense urban traffic and pollution around Piazza della Libertà. Impact on the structural stability of the monument cannot be excluded. In fact, the RADARSAT descending PS displacement maps show a localised deformation in the period 2003–2007 (Fig. 11A). The displacement trend in the time series shown in Fig. 11D is probably related to the damages of the basement of the monument which was repaired in

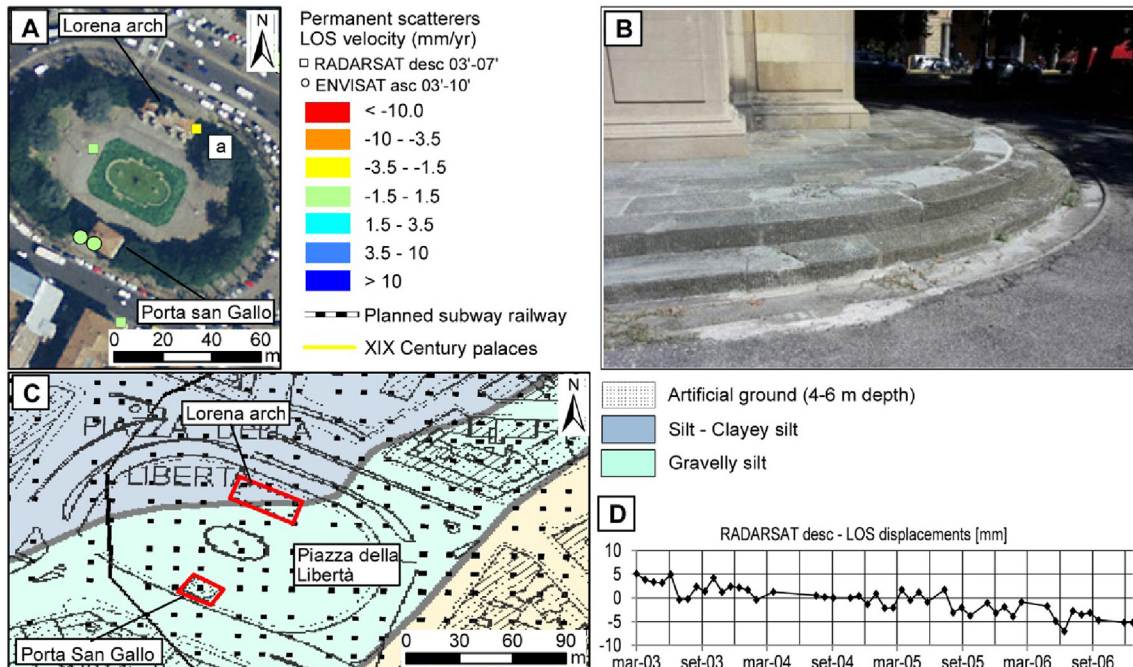


**Fig. 11.** (A) ENVISAT ascending 2003–2010 and RADARSAT descending 2003–2007 PS over Piazza della Libertà. (B) Detail of Lorena arch in correspondence of PS (a) in picture A. (C) Litotechnic map of Piazza della Libertà, scale 1:10,000 (Florence City Council, 2010). (D) Velocity plot of PS (a) in picture A.

the recent years (Fig. 11B).

It is a matter of conjecture whether these satellite evidences of damage can be correlated with the differential nature of the geological and anthropogenic deposits underneath the monument, as known from the litotechnic map 1:10,000 scale (Fig. 11C). Interestingly, this condition affects the Lorena arch but not Porta San Gallo. Therefore, this geological information needs to be accounted for specifically to understand possible differential structural behaviour of the arch in response to future excavations and stresses.

## 5. Conclusions

In the wider applied geographic literature and field practice which increasingly acknowledges the benefits of using remote sensing, the mapping procedure proposed in this article offers a novel rationale to exploit space-borne radar-based data. Building upon established methods of condition assessment at the scale of individual buildings (Pratesi et al., 2015; Tapete et al., 2015), a holistic method has been developed based on the decomposition of full sets of PSI measurements into velocity classes to enhance the patterns of urban changes and attribute them to different urban processes. For the first time, PS density is used not only to judge the reliability and accuracy of the interpretation of the deformation observed (Pratesi et al., 2015), but also as a mean by itself to identify urban dynamics due to demolitions of buildings, changes of urban land use and new areas of construction. In this regard our paper stands alone in the current literature.

The sensitivity of PSI technologies to millimetre-scale motions and large to local changes in urban land cover is proved suitable to detect the wide spectrum of phenomena related to the different aspects of urban evolution at multiple scales. Even in situations where field inspections would not be sufficient to recognize the occurrence of motions or surface changes due to the effect of urban sealing.

The implementation in Florence offers a catalogue of simple to complex urban dynamics that can be observed along the verticality and horizontality of transforming cities. The map of alert areas that we generated based on velocity decomposition maps at the various intervals of monitoring (mainly 1992–2000 and 2003–2010) not only showed the scale and boundaries of the effects due to the transition towards a metropolitan city and land surface processes occurred in the last 20 years but, more importantly, also provided evidence of differential conditions across the urban layout. North-western and south-western quarters are the hot spots of new building construction and regeneration projects for residential, business and tertiary service purposes. Exploitation and sustainable management of local groundwater resources emerge as one of the key issues there as the city expands. Conversely, the alert areas located in the southern and north-eastern sectors are symptoms of portions of the city where new urbanisation is limited and structural health issues of buildings are more due to local interactions with natural slope instability processes and underlying geology. This key evidence well summarizes the matter of fact relating to the physical geography of Florence. The gateways of the city to urban development are those that face westward, i.e. towards the open plain as the main source of land for new development.

The added value of such a historical analysis is the baseline characterisation of the urban environment before planned major infrastructure works take place. In this regard, Florence is an exemplar of how infrastructure is an asset towards a metropolitan character of a city, but at the same time an element that can impact on local buildings and heritage. Therefore it is envisaged that the evidence provided by our InSAR analysis will be essential to assess whether new monitoring campaigns would be able to pick up

motions associative with changed condition of the buildings in consequence of the infrastructure works.

From a technical point of view, further research advances may be to: (i) validate and extend the methodology to different urban contexts; (ii) exploit the high resolution, temporal coverage and sampling frequency of recent SAR satellites (e.g. RADARSAT-2, COSMO-SkyMed); (iii) verify the applicability of this approach with different InSAR processing techniques.

From a geographic perspective, the Florentine case study is a sample representing numerous situations of medium-size transforming cities across the world. Therefore this paper provides guidance on how to replicate the procedure of mapping and rating. It is also anticipated that the method can adapt to the scale of larger cities, even megacities where it is reasonable to expect higher number, magnitude and complexity of the urban dynamics. A crucial aspect will be the automation of some steps to increase the objectivity and rapidity of the analysis and classification of the patterns observed. In this sense development of software-aided methodologies is an open field.

## Acknowledgments

This research was led by F. Pratesi who developed the method and carried out the geospatial analysis in Florence with the contribution of D. Tapete. ERS-1/2 and ENVISAT ASAR PSI datasets used were accessed via the WMS service of the National Geoportal of the Italian Ministry of Environment, Territory and Sea, whereas RADARSAT-1 data were made available in the framework of DIANA project with Tuscany Region. The authors thank Prof. G. Pranzini for the insightful discussion about the hydrogeological setting of Florence.

## References

- Bateson, L., Cigna, F., Boon, D., & Sowter, A. (2015). The application of the Intermittent SBAS (ISBAS) InSAR method to the South Wales Coalfield, UK. *International Journal of Applied Earth Observation and Geoinformation*, 34, 249–257.
- Canuti, P., Casagli, N., Farina, P., Ferretti, A., Marks, F., & Menduni, G. (2005). Land subsidence in the Arno river basin studied through SAR interferometry. In *Proc. of SISOLS 2005, Seventh International Symposium on land subsidence* (Vol. 1, pp. 407–416). Shanghai, China, 23–28 October 2005.
- Castrenze, M., Nong, D., Tran, C., Young, L., & Fox, J. (2014). Mapping urban transitions using multi-temporal Landsat and DMSP-OLS night-time lights imagery of the Red River Delta in Vietnam. *Land*, 3(1), 148–166. <http://dx.doi.org/10.3390/land3010148>.
- Chatterjee, R. S., Fruneau, B., Rudant, J. P., Roy, P. S., Frison, P.-L., Lakhera, R. C., et al. (2006). Subsidence of Kolkata (Calcutta) city, India during the 1990s as observed from space by differential synthetic aperture radar interferometry (D-InSAR) technique. *Remote Sensing of Environment*, 102(1–2), 176–185. <http://dx.doi.org/10.1016/j.rse.2006.02.006>.
- Cigna, F., Bateson, L. B., Jordan, C. J., & Dashwood, C. (2014a). Simulating SAR geometric distortions and predicting Persistent Scatterer densities for ERS-1/2 and ENVISAT C-band SAR and InSAR applications: Nationwide feasibility assessment to monitor the landmass of Great Britain with SAR imagery. *Remote Sensing of Environment*, 152, 441–466.
- Cigna, F., Jordan, H., Bateson, L., McCormack, H., & Roberts, C. (2014b). Natural and anthropogenic geohazards in greater London observed from geological and ERS-1/2 and ENVISAT persistent scatterers ground motion data: Results from the EC FP7-SPACE PanGeo project. *Pure and Applied Geophysics*, 1–31. <http://dx.doi.org/10.1007/s00024-014-0927-3>.
- Cigna, F., Lasaponara, R., Masini, N., Miillo, P., & Tapete, D. (2014c). Persistent scatterer interferometry processing of COSMO-SkyMed StripMap HIMAE time series to depict deformation of the historic centre of Rome, Italy. *Remote Sensing*, 6, 12593–12618. <http://dx.doi.org/10.3390/rs61212593>.
- Cigna, F., Osmanoglu, B., Cabral-Cano, E., Dixon, T. H., Ávila-Olivera, J. A., Garduño-Monroy, V. H., et al. (2012). Monitoring land subsidence and its induced geological hazard with synthetic aperture radar interferometry: A case study in Morelia, Mexico. *Remote Sensing of Environment*, 117, 146–161. <http://dx.doi.org/10.1016/j.rse.2011.09.005>.
- Colesanti, C., Ferretti, A., Prati, C., & Rocca, F. (2001). Comparing GPS, optical leveling and permanent scatterers. In *Geoscience and remote sensing Symposium, 2001. IGARSS '01* (Vol. 6, pp. 2622–2624). Sydney: IEEE 2001 International. <http://dx.doi.org/10.1109/IGARSS.2001.978109>.
- Colesanti, C., & Wasowski, J. (2006). Investigating landslides with space-borne

- synthetic aperture radar (SAR) interferometry. *Engineering Geology*, 88(3–4), 173–199.
- Coli, M., Brugioni, M., & Montini, G. (2013). Florence and its floods: Anatomy of an hazard. In Proceeding of (Ed.), 18th International Conference on soil mechanics and Geotechnical Engineering (workshop of Geotechnical Engineering for conservation of cultural heritage and historical site), 7 pp.
- Costantini, M., Iodice, A., Magnapane, L., & Pietranera, L. (2000). Monitoring terrain movements by means of sparse SAR differential interferometric measurements. In *Proceedings IGARSS 2000 (IGARSS Honolulu)* (pp. 3225–3227).
- Crosetto, M., Monserrat, O., Jungner, A., & Crippa, B. (2009). Persistent scatterer interferometry: Potential and limits. In C. Heipke, K. Jacobsen, S. Müller, & U. Sörgel (Eds.), *ISPRS archives e Volume XXXVIII-1-4-7/W5, 2009, WG I/2, I/4, IV/2, IV/3, VII/2, ISPRS Hannover Workshop 2009, High-Resolution Earth Imaging for Geospatial Information, June 2–5, 2009 (Hannover, Germany)*.
- Dewan, A. M., & Yamaguchi, Y. (2009). Land use and land cover change in Greater Dhaka, Bangladesh: Using remote sensing to promote sustainable urbanization. *Applied Geography*, 29(3), 390–401. <http://dx.doi.org/10.1016/j.apgeog.2008.12.005>.
- Esch, T., Marconcini, M., Marmanis, D., Zeidler, J., Elsayed, S., Metz, A., et al. (2014). Dimensioning urbanization – An advanced procedure for characterizing human settlement properties and patterns using spatial network analysis. *Applied Geography*, 55, 212–228. <http://dx.doi.org/10.1016/j.apgeog.2014.09.009>.
- Fanti, R. (2006). Slope instability of San Miniato hill (Florence, Italy): Possible deformation patterns. *Landslides*, 3(4), 323–330.
- Faour, G., & Mhawej, M. (2014). Mapping urban transitions in the Greater Beirut area using different space platforms. *Land*, 3(3), 941–956. <http://dx.doi.org/10.3390/land3030941>.
- Ferretti, A., Prati, C., & Rocca, F. (2001). Permanent scatterers in SAR interferometry. *IEEE Transactions on Geoscience and Remote Sensing*, 39, 8e20. <http://dx.doi.org/10.1109/36.898661>.
- FIG. (2010). *Rapid urbanization and mega cities: The need for spatial information management*. International Federation of Surveyors. Research study by FIG Commission 3. FIG Publication no. 48, 90 pp. ISBN 978-87-90907-78-5. Accessed at <http://www.fig.net/pub/figpub/pub48/figpub48.pdf>.
- Florence City Council. (2010). *Piano strutturale*. Available at: <http://pianostrutturale.comune.fi.it>.
- Florence City Council. (2015a). <http://www.passantefirenze.it/>.
- Florence City Council. (2015b). [http://mobilita.comune.fi.it/tramvia/sistema\\_tramviario/linea2.html](http://mobilita.comune.fi.it/tramvia/sistema_tramviario/linea2.html).
- Florence City Council. (2015c). <http://prg.comune.fi.it/>.
- Florence Province. (2014). <http://mappe.provincia.fi.it/tolomeo/html/servizi/pozzi/mappapozzi.html>.
- Haas, J., Furberg, D., & Ban, Y. (2015). Satellite monitoring of urbanization and environmental impacts—A comparison of Stockholm and Shanghai. *International Journal of Applied Earth Observation*, 38, 138–149. <http://dx.doi.org/10.1016/j.jag.2014.12.008>.
- ISTAT. (2014). *Popolazione Residente per età, sesso e stato civile al 1° gennaio 2014*. Accessed at: <http://demo.istat.it/>.
- Kontogi, C., Schneider, A., Fox, J., Saksena, S., Spencer, J. H., & Castrenze, M. (2014). Monitoring peri-urbanization in the greater Ho Chi Minh City metropolitan area. *Applied Geography*, 53, 377–388. <http://dx.doi.org/10.1016/j.apgeog.2014.06.029>.
- Lu, P., Casagli, N., & Catani, F. (2010). PSI-HSR: A new approach of representing Persistent Scatterer interferometry (PSI) point targets using hue and saturation scale. *International Journal of Remote Sensing*, 31, 2189–2196.
- Mirri, S., & Sargentini, M. (2005). Tunnelling and environmental protection: The experience of the Bologna-Florence high speed rail line. In *Géoline 2005 – Lyon, France – 23rd - 25th May/Mai 2005*, 7 pp. Accessed at <http://www.geotech-fr.org/sites/default/files/congres/geoline/GEOLINE2005%20S12%20pp%201-7%20Mirri.pdf>.
- Morelli, S., Battistini, A., & Catani, F. (October 2014). Rapid assessment of flood susceptibility in urbanized rivers using digital terrain data: Application to the Arno river case study (Firenze, northern Italy). *Applied Geography*, 54, 35–53. <http://dx.doi.org/10.1016/j.apgeog.2014.06.032>. ISSN 0143-6228.
- Perissin, D., Wang, Z., & Lin, H. (2012). Shanghai subway tunnels and highways monitoring through Cosmo-SkyMed Persistent Scatterers. *ISPRS Journal of Photogrammetry and Remote Sensing*, 73, 58–67.
- Pranzini, G. (2008). *Idrogeologia della piana fiorentina. Conference "Un piano per la Piana. idee e progetti per un parco"*. Florence, Italy, 9–10 May 2008 <http://www2.msn.unifi.it/upload/sub/specola/img/Piano%20per%20la%20piana/piana03.pdf>.
- Pratesi, F., Tapete, D., Terenzi, G., Del Ventisette, C., & Moretti, S. (2015). Rating health and stability of engineering structures via classification indexes of InSAR Persistent Scatterers. *International Journal of Applied Earth Observation*, 40, 81–90. <http://dx.doi.org/10.1016/j.jag.2015.04.012>.
- Righini, G., Pancioli, V., & Casagli, N. (2012). Updating landslide inventory maps using Persistent Scatterer Interferometry (PSI). *International Journal of Remote Sensing*, 33(7), 2068–2096.
- Romero-Lankao, P., & Dodman, D. (2011). Cities in transition: Transforming urban centers from hotbeds of GHG emissions and vulnerability to seedbeds of sustainability and resilience: Introduction and editorial overview. *Current Opinion in Environmental Sustainability*, 3(3), 113–120. <http://dx.doi.org/10.1016/j.cosust.2011.02.002>.
- Saksena, S., Fox, J., Spencer, J., Castrenze, M., DiGregorio, M., Epprecht, M., et al. (June 2014). Classifying and mapping the urban transition in Vietnam. *Applied Geography*, 50, 80–89. <http://dx.doi.org/10.1016/j.apgeog.2014.02.010>. ISSN 0143-6228.
- Samsonov, S. V., d'Oreye, N., González, P. J., Tiampo, K. F., Ertolahti, L., & Clague, J. J. (2014). Rapidly accelerating subsidence in the Greater Vancouver region from two decades of ERS-ENVISAT-RADARSAT-2 DInSAR measurements. *Remote Sensing of Environment*, 143(5), 180–191. <http://dx.doi.org/10.1016/j.rse.2013.12.017>.
- Stabel, E., & Fischer, P. (2001). Satellite radar interferometric products for the urban application domain. *Advances in Environmental Research*, 5(4), 425–433. [http://dx.doi.org/10.1016/S1093-0191\(01\)00094-6](http://dx.doi.org/10.1016/S1093-0191(01)00094-6).
- Stramondo, S., Bozzano, F., Marra, F., Wegmüller, U., Cinti, F. R., Moro, M., & Saroli, M. (2008). Subsidence induced by urbanisation in the city of Rome detected by advanced InSAR technique and geotechnical investigations. *Remote Sensing of Environment*, 112(6), 3160–3172. <http://dx.doi.org/10.1016/j.rse.2008.03.008>.
- Su, S., Xiao, R., & Zhang, Y. (March 2012). Multi-scale analysis of spatially varying relationships between agricultural landscape patterns and urbanization using geographically weighted regression. *Applied Geography*, 32(2), 360–375. <http://dx.doi.org/10.1016/j.apgeog.2011.06.005>. ISSN 0143-6228.
- Tapete, D., & Cigna, F. (2012a). Rapid mapping and deformation analysis over cultural heritage and rural sites based on persistent scatterer interferometry. *International Journal of Geophysics*, 2012. <http://dx.doi.org/10.1155/2012/618609>. Article ID 618609, 19 pp.
- Tapete, D., & Cigna, F. (2012b). Site-specific analysis of deformation patterns on archaeological heritage by satellite radar interferometry. In *20th International materials research Congress, Symposium 8 cultural heritage and Archaeological issues in materials Science, MRS Proceedings* 1374 (pp. 283–295). Cambridge University Press. <http://dx.doi.org/10.1557/opl.2012.1397>, 2012.
- Tapete, D., Fanti, R., Cecchi, R., Petrangeli, P., & Casagli, N. (2012). Satellite radar interferometry for monitoring and early-stage warning of structural instability in archaeological sites. *Journal of Geophysics and Engineering*, 9(4), S10eS25. <http://dx.doi.org/10.1088/1742-2132/9/4/S10>.
- Tapete, D., Morelli, S., Fanti, R., & Casagli, N. (2015). Localising deformation along the elevation of linear structures: An experiment with space-borne InSAR and RTK GPS on the Roman Aqueducts in Rome, Italy. *Applied Geography*, 58, 65–83. <http://dx.doi.org/10.1016/j.apgeog.2015.01.009>.
- Terranova, C., Ventura, G., & Vilardo, G. (2015). Multiple causes of ground deformation in the Napoli metropolitan area (Italy) from integrated Persistent Scatterer DinSAR, geological, hydrological, and urban infrastructure data. *Earth-Science Reviews*, 146, 105–119. <http://dx.doi.org/10.1016/j.earscirev.2015.04.001>.
- Terzaghi, K., & Peck, R. B. (1967). *Soil mechanics in engineering practice*. John Wiley and Sons.
- Toc Toe Firenze. 2015. <http://www.toctocfirenze.it/tramvia-palazzo-mazzoni/>.
- Tuscany Region. 2006. <http://www.lamma.rete.toscana.it/inventario-fenomeni-franosi-italiani-ififi-regione-toscana>.
- Tuscany Region. 2014. <http://www.regione.toscana.it/-/cartografia-tecnica-regionale-e-scarico-dati-geografici>.
- Zhang, Q., & Seto, K. C. (2011). Mapping urbanization dynamics at regional and global scales using multi-temporal DMSP/OLS night time light data. *Remote Sensing of Environment*, 115(9), 2320–2329. <http://dx.doi.org/10.1016/j.rse.2011.04.032>.
- Zong-Guo, X., & Henderson, F. M. (1997). Understanding the relationships between radar response patterns and the bio- and geophysical parameters of urban areas. *Geoscience and Remote Sensing IEEE Transactions on*, 35(1), 93–101. <http://dx.doi.org/10.1109/36.551938>.